Title: Retrieval of SO_2 columns from FY3F/OMS instrument observations

Authors: Huanhuan Yan, Andreas Richter, Xingying Zhang, Anja Schönhardt, Thomas Visarius, Qian Wang, Lu Zhang, Yichen Li, Chao Yu, Weihe Wang

---

We sincerely thank the AMT Editors and all the anonymous Referees for handling the review process, carefully reading our manuscript, and providing constructive comments. The paper was corrected according to the suggestions of the Editors and the Referees. We hope that in dealing with the comments put forward by Anonymous Referees, the overall quality of the manuscript was improved. We addressed the comments below.

Response to the Editor's Comments

1. **Comment:** Section "Author contribution": please use initials instead of full author names, i.e. "HY" instead of "Huanhuan Yan".

   Response: Thank the Editor for pointing this out. The Author Contribution section has been revised in the updated manuscript, and all author names are now listed using initials (e.g., HY instead of Huanhuan Yan). In addition, we would like to note that during the revision process, we received valuable assistance from Qian Wang, Lu Zhang, Yichen Li, Chao Yu, and Weihe Wang. Therefore, their names have been added to the list of co-authors in the revised manuscript. Please refer to the updated manuscript for details.

Response to Referee #3

We sincerely thank Referee #3 for the valuable comments and suggestions, which have significantly improved the quality of the manuscript. In response to these comments, substantial revisions have been made, which took more than three months to complete. The major revisions mainly include two aspects: (1) the AMFs were recalculated using the radiative transfer model SCIATRAN combined with SO_2 profiles from GEOS-CF, and the corresponding figures, descriptions, and conclusions were updated accordingly; and (2) the error analysis section was almost rewritten to provide a quantitative assessment of the impacts of individual error sources and the overall uncertainties of OMS SO_2 VCD. Below, we respond to each comment in detail.

1. **Comment:** Figures 2 and 3: The discussion appears more focused on justifying methodological choices rather than contributing substantive value to the present work. Moreover, the analysis is based on a single day, lacking statistical support. I suggest summarizing these results concisely and clearly stating that the 312-326 nm range is used for the current retrieval.

   Response: We thank the reviewer for this comment and agree with the suggestion.

   To present the selection of the 312–326 nm fitting window more concisely and clearly, Section 3.3.1 has been revised in both text and figures.

   (1) Text revisions:

   The discussion previously focused on justifying methodological choices has been significantly shortened. A concise and clear explanation supporting the selection of the 312–326 nm fitting window is now provided in the revised manuscript, and the descriptions of comparisons between different fitting windows have been simplified. Overall, the length of Section 3.3.1 has been reduced from 39 lines to 22 lines in the revised manuscript. For detailed modifications, please refer to Section 3.3.1 in the revised manuscript.

   (2) Figures and tables:

   Since Table 2 and Figures 2 and 3 in the previous revised manuscript mainly served to justify the fitting window selection rather than contribute substantive scientific results, they have been removed together with the corresponding textual descriptions in the revised manuscript.

   (3) Response to comment “the analysis is based on a single day, lacking statistical support”.

   We agree that fitting window selection is critical for SO_2 retrieval. In this study, we collected the fitting windows commonly used in published SO_2 retrieval algorithms (previously listed in Table 2) and evaluated these windows using OMS data. However, this approach does not yet represent an optimal

wavelength selection strategy.

A comprehensive statistical evaluation over multiple atmospheric conditions and multiple OMS orbits is necessary to further identify and validate the optimal fitting window. However, including multi-orbit and multi-day comparisons across different fitting windows would require a substantial number of additional figures and pages. As this study primarily aims to present the first OMS SO_2 retrieval results, further systematic evaluations of retrieval performance using different fitting windows will be conducted in future work. Specifically, we plan to 1) perform forward radiative transfer simulations under various atmospheric and surface conditions to assess errors from different fitting windows, and 2) apply the selected fitting windows to multi-orbit, multi-day OMS observations over different regions to quantitatively evaluate the robustness of the fitting window choice. This issue will be addressed in a dedicated follow-up study.

2. **Comment:** Figure 4: All tested wavelength ranges fall outside the 312–326 nm region, and no narrower intervals (e.g., 315–325 nm) were explored. Please clarify this choice. Additionally, it would strengthen the analysis to include a comparison with TROPOMI SO_2 retrievals to evaluate the consistency in magnitude and better validate the selected wavelength range.

Response: Thank the reviewer for this comment. Before addressing the detailed responses below, we would like to note that, Table 2 and Figures 2–3 in the previous version have been removed for clarity in the revised manuscript. Consequently, the previous Figure 4 is now Figure 2 in the revised manuscript.

(1) Response to "All tested wavelength ranges fall outside the 312–326 nm region, and no narrower intervals (e.g., 315–325 nm) were explored. Please clarify this choice".

The revised Figure 2 includes results using 312–326 nm fitting window.

Regarding the reviewer's example of the 315–325 nm interval, we are not certain whether this refers to the fitting windows (e.g., 312–326 nm or 315–327 nm) that were already tested and presented in the previous manuscript (Figures 2 and 3).

If this is the case, the reasons are 1) only a representative subset of fitting windows was displayed to maintain clarity and avoid excessive overlap among multiple curves, and 2) the OMS SO_2 retrievals from 312–326 nm or 315–327 nm window exhibited relatively large errors in clean regions (e.g., OMS cross-track positions 1–150), as shown in the previous Figures 2 and 3.

If this is not the case, we would like to clarify that we did not attempt an exhaustive exploration of every possible fitting window in this study. Instead, we collected the fitting windows commonly used in

published SO_2 retrieval algorithms (previously listed in Table 2) and evaluated these windows using OMS data. We acknowledge that a comprehensive statistical evaluation over multiple atmospheric conditions and multiple OMS orbits is necessary to further validate the optimal fitting window selection. Due to the substantial work required for such an analysis, this has been planned as future work, as described in our response to Comment 1.

(2) Response to "Additionally, it would strengthen the analysis to include a comparison with TROPOMI SO_2 retrievals to evaluate the consistency in magnitude and better validate the selected wavelength range".

Thank the reviewer's suggestion to use the TROPOMI as a reference dataset to evaluate the consistency in magnitude and validate the selected fitting window. TROPOMI provides highly sensitive detection of volcanic SO_2 emissions and has been widely used in eruption events.

However, the true SO_2 column at the exact satellite overpass time during volcanic events is difficult to obtain, and TROPOMI SO_2 retrievals over volcanic regions still involve considerable uncertainties (Theys et al., 2017; Hedelt et al., 2019). Therefore, using TROPOMI as a strict reference for validating the suitability of specific fitting windows may not be fully appropriate.

In addition, the results presented in this section focus on SO_2 SCDs. Due to differences in viewing geometry between OMS and TROPOMI, SCDs are not directly comparable. A comparison based on VCDs would further involve different uncertainties from AMF calculations, making it difficult to isolate the impact of fitting window selection from AMF-related effects.

In this study, the selection of fitting windows was mainly based on three considerations: (a) consistency with fitting windows commonly used in the published SO_2 retrieval algorithms; (b) windows yield SO_2 retrievals close to zero over clean regions, with low standard deviations and mean values; (c) windows provide high SO_2 values within the volcanic plume. Based on these criteria, the 312–326 nm window represents a reasonable choice for OMS SO_2 retrievals.

We acknowledge that the 312–326 nm fitting window may not represent the optimal choice under all conditions. A comprehensive statistical evaluation over multiple atmospheric scenarios and multiple OMS orbits is required to further validate the optimal fitting window selection. Moreover, the optimal fitting window may vary with SO_2 loading, particularly under strong volcanic eruption conditions, where absorption saturation may occur and lead to underestimation of SO_2 columns.

We plan to conduct a detailed analysis of fitting window selection for OMS SO_2 retrievals in future work. We appreciate the reviewer for pointing this out.

3. **Comment:** Section 3: I agree with previous reviewers that the manuscript includes several subjective explanations already well documented in literature (e.g., detailed Ring effect discussion).

Response: Thanks for pointing this out, and we apologize for the subjective or redundant explanations included in the previous version of the manuscript. Following the reviewer's suggestion, we have removed or shortened text in section 3.

Below we list some major revisions, while additional minor revisions (such as wording adjustments and small changes in sentence structure) can be found in the revised manuscript and in the track changes file.

(1) In the first paragraph of Section 3, we have condensed the detailed description of the OMS SO_2 retrieval steps and retained only a concise overview of the main procedures. The original text (shown in blue font) has been revised to the updated version (shown in red font).

The SO_2 retrieval from FY3F/OMS mainly involves the following steps. (1) The OMS-N L1 earth radiance is normalized to the Earth-Sun distance of 1AU, while the solar irradiance is obtained by convolving the Total and Spectral Solar Irradiance Sensor (TSIS) Hybrid Solar Reference Spectrum (HSRS) (Coddington et al., 2021) (See section 3.1 for more information) with the Instrument Spectral Response Function (ISRF) of OMS-N. (2) The 312-326 nm region is chosen as the retrieval fitting window of the OMS SO_2 column. (3) Spectral soft calibration is performed using the absorption peaks and valleys of the solar reference spectrum. (4) The cross sections of SO_2 and O_3 in 312-326 nm are convolved with the ISRF. (5) The Ring spectrum is calculated using the SCIATRAN Radiative Transfer Model (Rozanov et al., 2005). (6) SO_2, O_3 and Ring cross-sections together with a third-order polynomial are used in the DOAS fitting process to obtain the SCD of OMS SO_2. (7) The AMF is applied to get vertical column density (VCD). (8) A specific correction scheme for OMS background offset is applied to effectively reduce along-track stripes and across-track asymmetries in the initial OMS SO_2 retrievals.

The SO_2 retrieval from FY-3F/OMS involves radiance normalization, spectral soft calibration, convolution of SO_2 and O_3 cross-sections and Ring spectrum with the OMS-N Instrument Spectral Response Function (ISRF), DOAS fitting to obtain SO_2 SCD, AMF conversion to vertical column density (VCD), and background offset correction to reduce striping and across-track asymmetries.

(2) Section 3.1. The ISRF is not a focus of this study and has already been described in detail in Wang et al. (2024). To avoid providing explanations that are already well documented in the literature, we have removed the following content from Section 3.1 of the original manuscript (shown in blue).

The FY3F/OMS-N ISRF was determined using tunable laser scanning with a step size of 0.02 nm, providing the relative response of each detector pixel on the focal plane arrays to monochromatic illumination (Wang et al., 2024). It varies in both the spectral and spatial dimensions of the two large array detectors. The shape of the FY3F/OMS-N ISRF exhibits a flat top in the central peaks because OMS-N adopts a stereoscopic slit observation mode (Wang et al., 2024). The TSIS HSRS hybrid solar reference spectrum provides high accuracy solar irradiances, but as it was not measured with the OMS-N instrument, any calibration issues in the radiances do not cancel in the DOAS retrieval. Therefore, its use may lead to systematic overestimation or underestimation in the retrieved SO_2 columns, as well as along-track stripes, which cannot be fully corrected through post-processing algorithms.

(3) Section 3.3.1. As mentioned in our response to Comment 1, and following the reviewer's suggestion to concisely and clearly state the selection of the fitting window for the OMS SO_2 retrieval, we have

condensed the content of this section. To avoid duplication in the response letter, please refer to our response to Comment 1 as well as the revised manuscript and the tracked-changes file for the detailed modifications.

(4) Section 3.3.2. The description of the Ring effect in Section 3.3.2 has also been condensed. The original text (shown in blue) has been revised to the updated version (shown in red).

The Ring effect refers to the phenomenon that the Fraunhofer lines present in the solar spectrum from absorption in the solar atmosphere by elements such as potassium and calcium are partially filled in spectra of scattered light taken in the Earth's atmosphere (Grainger and Ring, 1962). For the Ring effect in satellite-observed spectra, the primary source is the rotational Raman scattering of N2 and O2 molecules in the atmosphere, which redistributes photon energy and leads to the filling-in of Fraunhofer and atmospheric absorption lines (Sioris and Evans, 1999; Fish and Jones, 1995; Chance and Spurr, 1997; Vountas et al., 1998). For OMS SO2 column retrievals using the DOAS method, the Ring effect is an important factor influencing the accuracy of retrieval results due to the strong Ring spectrum in the UV wavelength band (Fig. 5). Taking the OMS 20240823_1036 orbit as an example, after including the Ring spectrum into the DOAS retrieval, the spectral fitting residual RMSE for most OMS pixels decreases by approximately 0.004 to 0.01.

The Ring effect is an important factor influencing the accuracy of SO_2 retrieval results due to the pronounced filling-in features of the Ring spectrum in the UV region (Fig. 3). It redistributes photon energy and leads to the filling-in of Fraunhofer and atmospheric absorption lines (Sioris and Evans, 1999; Fish and Jones, 1995; Chance and Spurr, 1997; Vountas et al., 1998).

4. **Comment:** You earlier compared wavelength choices thoroughly, yet in the Ring effect section, you mention using fixed input values "used in the DOAS fitting for all OMS measurements, without considering the variations of the Ring spectrum due to different atmospheric conditions and viewing geometries." Does this imply those variations have minimal influence on your retrieval or slant columns (SCDs)? Please clarify.

Response: We thank the reviewer for this comment and apologize for the unclear expression in the manuscript. Our response is as follows:

(1) We acknowledge that the Ring effect in DOAS retrievals varies with atmospheric conditions and viewing geometries. A sensitivity analysis has been conducted and is presented in Section 5.1.3 and Figure 17 in the revised manuscript. The Ring spectrum was calculated using the SCIATRAN model and convolved with the OMS ISRF to investigate its variation with O_3, VZA, SZA, and surface reflectivity (AS).

(2) The rationale for using a fixed Ring spectrum in the OMS SO_2 retrieval and the corresponding revisions made in the revised manuscript to enhance clarity.

The Ring effect is a non-negligible component in the UV DOAS SCD fitting process. In principle, using a Ring spectrum that varies with input conditions could provide more accurate OMS SO_2 retrievals.

Initially, we generated a lookup table of Ring spectra for the 310–330 nm wavelength range using the SCIATRAN model, considering variations in SZA, VZA, O_3 column, and AS to achieve more accurate retrievals. However, in practice, this lookup table was very large and significantly increased the computational cost for OMS SO_2 retrievals. More importantly, although the Ring spectrum exhibits noticeable variability with SZA, VZA, O_3, and AS within the 310–330 nm range, its influence on the retrieved OMS SO_2 slant column densities was found to be relatively small (<3% or less). This is mainly due to the weak correlation between the Ring spectrum and the satellite TOA reflectance, especially in the case of volcanic eruptions with high SO_2 concentrations.

To verify this, we conducted two sensitivity tests using OMS orbit 20240823_1036, which includes both strong volcanic SO_2 signals and clean ocean regions (please see the two figures below). In the first test, only the solar zenith angle (SZA = 0° and 70°) was varied, while all other parameters were fixed. In the second test, only the surface reflectivity (AS = 0.05 and 0.8) was varied. The results confirm that although the Ring spectrum changes with viewing geometry and surface reflectivity, its impact on the retrieved OMS SO_2 SCDs remains small.

Based on these findings, we adopted a fixed Ring spectrum simulated with SCIATRAN for all OMS retrievals. For clarity, in the revised manuscript, the original text at the end of Section 3.3.2 (shown in blue) has been replaced with the updated text (shown in red).

Note that in this study the SCIATRAN Ring spectrum for typical atmospheric conditions and observational geometry (SZA=30°, Viewing Zenith Angle (VZA)=0°, Relative Azimuth Angle (RAA)=0°, surface reflectance (AS)=0.05, surface height above sea level (HS) (also referred to as terrain height)=0 km, ozone column=275 DU, clear sky) is used in the DOAS fitting for all OMS measurements, without considering the variations of the Ring spectrum due to different atmospheric conditions and viewing geometries.

Note that in this study a fixed Ring spectrum calculated using the SCIATRAN model under typical atmospheric and surface conditions and observational geometry (SZA=30°, Viewing Zenith Angle (VZA)=0°, Relative Azimuth Angle (RAA)=0°, surface reflectance (AS)=0.05, surface height above sea level (HS) (also referred to as terrain height)=0 km, ozone column=275 DU, clear sky) is used in the DOAS fitting for all OMS measurements. Variations of the Ring spectrum due to different atmospheric conditions and viewing geometries are not considered, since applying the Ring lookup table would be computationally costly and its impact on OMS SO_2 SCD retrievals is limited. A detailed error analysis of this fixed Ring approach is discussed in Section 5.1.3.

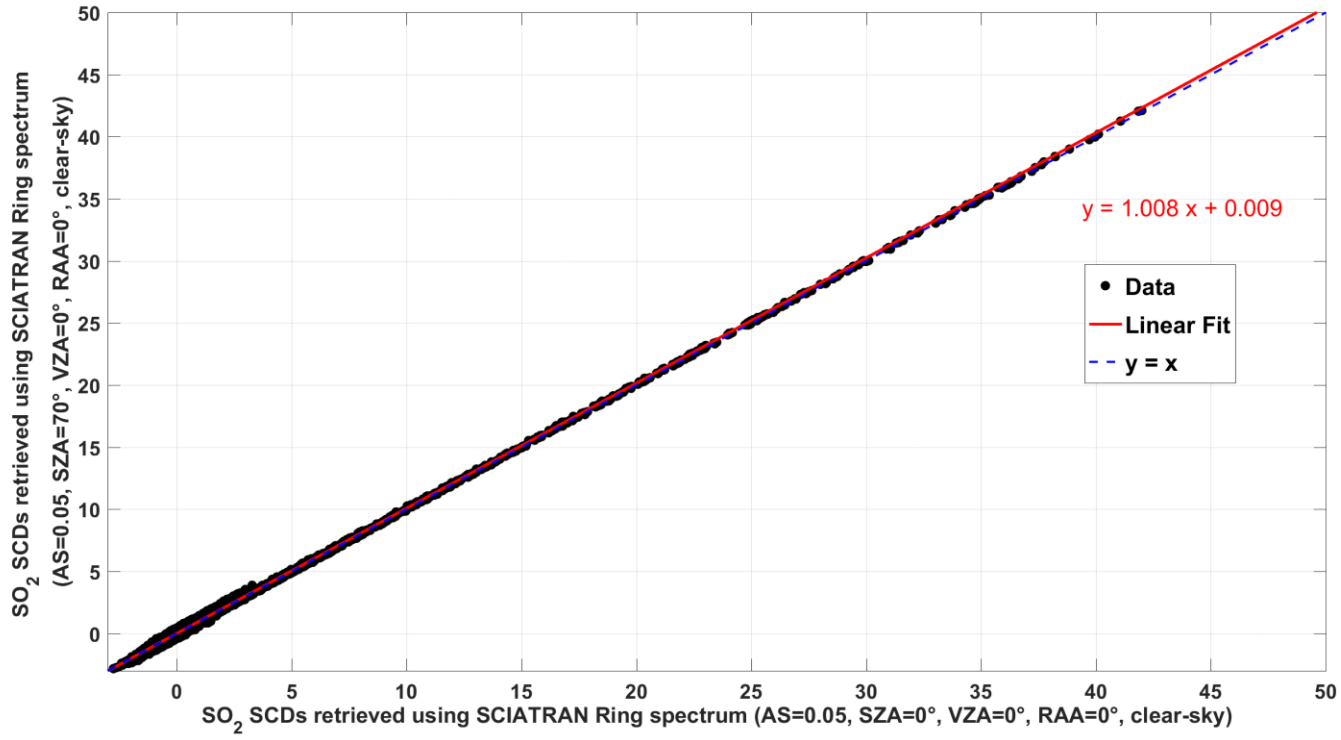

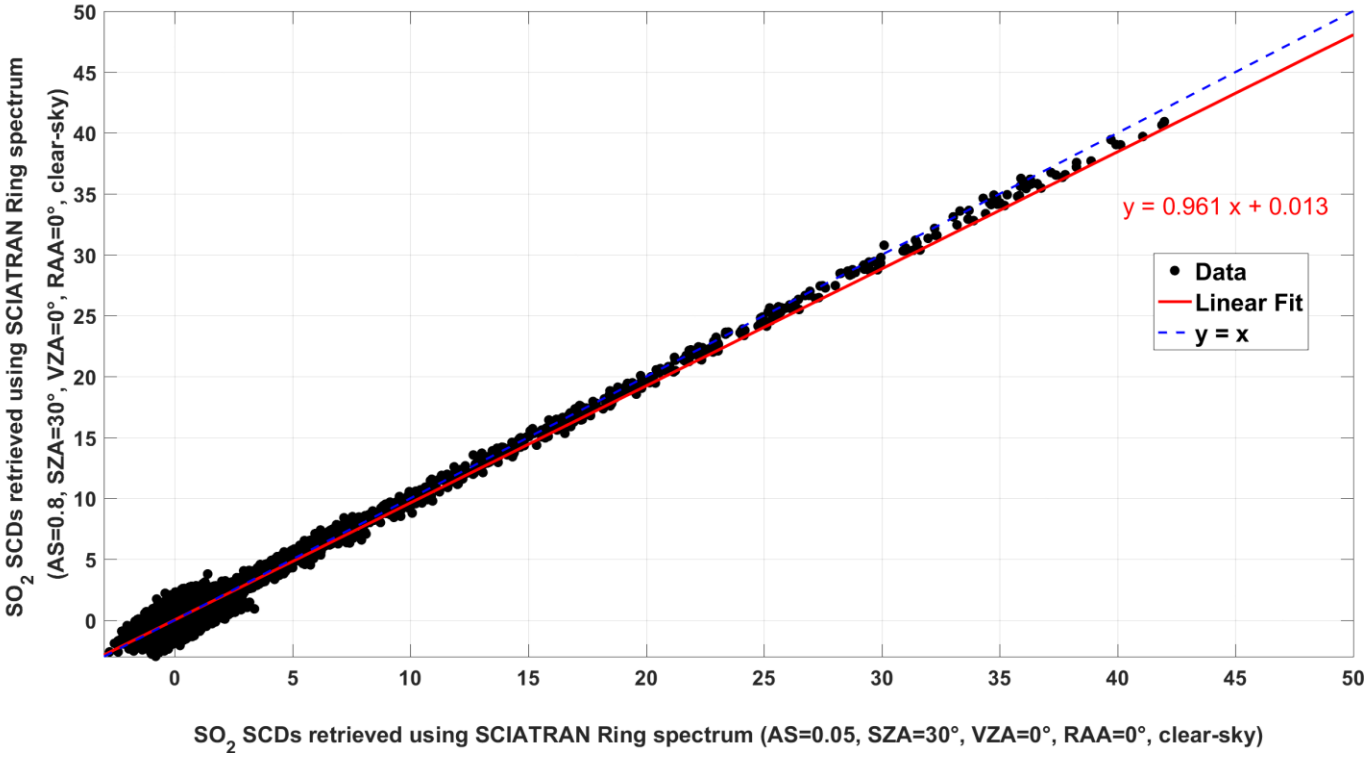

(3) Future improvements

We acknowledge that incorporating variable Ring spectra may further improve retrieval accuracy under certain extreme conditions. In future work, we plan to further investigate the sensitivity of OMS SO_2 retrievals to Ring spectrum variability and, if necessary, incorporate this effect into the retrieval algorithm.

5. **Comment:** Section 4.5: What are the typical scattering weights or averaging kernels (AKs) of OMS SO_2 retrievals?

Response: Thank the reviewer for this comment.

The scattering weights or averaging kernels (AKs) quantify the vertical sensitivity of satellite retrieval to changes in the true atmospheric profile. In practice, it cannot be measured directly from satellite observations, but can be accurately simulated using a radiative transfer model. For consistency with previous studies on TROPOMI SO_2 retrievals (Theys et al., 2017), here we focus on averaging kernels (AKs) rather than scattering weights. As described in Burrows, Platt, and Borrell (2011) and Eskes & Boersma (2003), the AKs can be calculated as:

$$AK_i = \frac{Box\text{-}AMF_i}{AMF}$$

where $Box\text{-}AMF_i$ is the box air mass factor for layer i and AMF is the total air mass factor. As described in Section 3.4 of the revised manuscript, the AMF is computed as a weighted average of the altitude-dependent Box-AMFs across all layers, with the weights determined by the SO_2 distribution in each layer (Chen et al., 2009; Wagner et al., 2007; Palmer et al., 2001; Boersma et al., 2004):

$$\mathrm{AMF} = \sum_{\mathrm{i}} \mathrm{Box\text{-}AMF_i} \times \frac{\mathrm{c_i} \cdot \Delta \mathrm{h_i}}{\sum_{\mathrm{j}} \mathrm{c_j} \cdot \Delta \mathrm{h_j}}$$

Where $\mathrm{c_i}$ represents the SO_2 number density in the i-th layer, and $\Delta \mathrm{h_i}$ denotes the thickness of that layer. It is interesting to note here, that for optically thin absorbers (optical depth <<1), the box-AMFs are identical to the so called weighting functions (Rodgers, 1976, 2000).

From the AK definition above, the averaging kernels of OMS SO_2 retrievals depend primarily on the instrument viewing geometry (SZA, VZA, RAA), surface reflectance, and the SO_2 vertical profile (because the AMF computation requires an a-priori profile). We calculated representative AKs under typical viewing and surface conditions (SZA = 30°, VZA = 0°, RAA = 0°, surface albedo = 0.05, surface altitude = 0 km, clear sky), using an assumed anthropogenic SO_2 profile with a total column of approximately 10 DU. As shown in the figure below, the typical OMS SO_2 AKs indicate (1) a maximum sensitivity in the mid–upper troposphere, with the peak generally located around 10–15 km, and (2) reduced sensitivity in the boundary layer, consistent with the weak near-surface sensitivity of UV backscatter instruments.

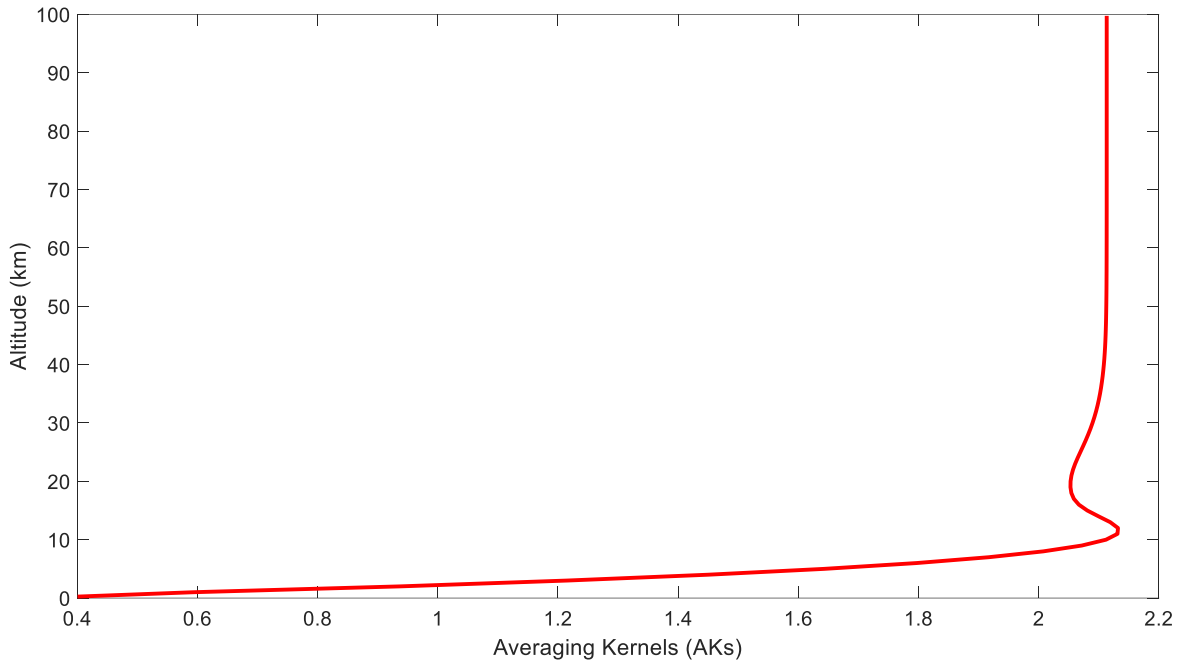

6. Comment: Your use of constant AMFs simply scales the data linearly. If vertical profiles are unavailable, model-based profiles (or at minimum, geometric AMFs) should be considered, a common practice in such retrievals. You refer to Section 5.2 for AMF and error details, but this section primarily describes RTM runs under various settings without quantitative error estimates relevant to your retrieval. A more robust discussion of structural uncertainties is needed.

Response: Thank the reviewer for this constructive comment and suggestion. For clarity, we divide the above comment into two parts and address them separately below.

- **Response to comment "Your use of constant AMFs simply scales the data linearly. If vertical profiles are unavailable, model-based profiles (or at minimum, geometric AMFs) should be considered, a common practice in such retrievals."**

We agree with the reviewer that the use of constant AMFs simply scales the retrieved SO_2 linearly and can introduce substantial uncertainty. Following the reviewer's suggestion, we made effort in this revision to improving the AMF treatment and have revised both Section 3.4 (AMF calculation) and Section 5.2 (AMF uncertainty analysis), including updated descriptions and newly added figures and tables.

We explored two alternative AMF approaches in addition to the simplified constant AMF scheme. The first approach employs geometric AMFs (hereafter referred to as AMFgeo) to convert OMS SO_2 SCDs to VCDs. The second approach uses model vertical SO_2 profiles combined with radiative transfer modeling to derive RTM-based AMFs. The two approaches are described in detail below.

(1) AMFgeo

Under the assumption of a plane-parallel atmosphere without considering scattering effects, the geometric AMF is calculated based on the observation geometry using an empirical formula:

$$\mathrm{AMF} \approx \mathrm{AMFgeo} = cos^{-1}\theta_s + cos^{-1}\theta_v$$

where AMFgeo denotes the geometric AMF, θ_s is the solar zenith angle, and θ_v is the satellite viewing zenith angle. This formulation is commonly applied in cases where fast VCD estimation is needed.

Using the OMS solar zenith and viewing angles, we calculated AMFgeo and converted OMS SO_2 SCDs into VCDs accordingly. Due to the large number of figures, the resulting SO_2 columns derived using AMFgeo are provided in Supplement-1, which is included at the end of this document. As shown in the figures of the Supplement-1, AMFgeo exhibits a spatial pattern characterized by lower values near the center of the orbit and higher values toward the swath edges, with typical magnitudes generally exceeding 2. These values are largely higher than AMFs derived from radiative transfer modeling under typical atmospheric and surface conditions. Consequently, the application of geometric AMFs leads to lower OMS SO_2 columns. Over oceanic regions, the retrieved OMS SO_2 columns approach zero more closely and show a markedly reduced standard deviation, while over high-concentration regions the SO_2 values become much lower and are significantly smaller than those retrieved by the TROPOMI DOAS and COBRA products.

Therefore, considering the large uncertainties associated with AMFgeo, this approach was not adopted for OMS SO_2 VCD calculation in the revised manuscript.

(2) RTM-based AMF

The RTM-based AMF approach is adopted in the revised manuscript. RTM-based AMFs require high-resolution global SO_2 vertical profiles as input. We initially examined the climatological model-based profile database provided within SCIATRAN, which is organized by month and latitude. Although these files include SO_2 profiles, they were found to be identical across different months and latitude ranges, effectively representing only a single clean-background SO_2 profile.

Subsequently, we obtained SO_2 vertical profile data from the GEOS-CF system available through the NASA Center for Climate Simulation (NCCS), with a horizontal resolution of 0.25° × 0.25°, a temporal resolution of 1 hour, and 72 vertical model layers extending up to 0.01 hPa. These GEOS-CF profiles were then used to compute RTM-based AMFs.

We calculated RTM-based AMFs using SO_2 vertical profiles from GEOS-CF in combination with BoxAMFs derived from the SCIATRAN radiative transfer model. These RTM-based AMFs were then applied to convert OMS SO_2 SCDs into VCDs, and the corresponding updated results have been included

in the revised manuscript. More comparisons among OMS SO_2 SCDs, OMS SO_2 VCDs using RTM-based AMFs, TROPOMI DOAS SO_2, and TROPOMI COBRA SO_2 are provided in Supplement-2, which is included at the end of this document. It is worth noting that, in the revised manuscript, OMS SO_2 SCDs are not included in the comparisons.

Although GEOS-CF provides vertical profile inputs for the RTM-based AMF calculations, the accuracy of the GEOS-CF SO_2 profiles remains uncertain. As reported in Keller et al. (2021), which describes the GEOS-CF v1.0 system:

> *"Comparisons against surface observations highlight the successful representation of air pollutants in many regions of the world and during all seasons, yet also highlight current limitations, such as a global high bias in SO_2..."*
> *"For SO_2, the model–observation comparison shows a large model bias of up to a factor of 4, with an annual mean bias of 2.1 at GAW sites and 1.5 at OpenAQ locations."*
> *"GEOS-CF v1.0 systematically overpredicts SO_2 due to the use of outdated emissions data..."*

Therefore, the adoption of GEOS-CF model-based profiles for OMS SO_2 AMF computation may introduce additional uncertainties, particularly for episodic events such as volcanic eruptions.

Overall, regardless of the AMF strategy adopted (constant, geometric, or RTM-based), the accuracy of the OMS SO_2 retrievals was not be fully evaluated due to the lack of ground-based SO_2 observations. In the future, ground-based and airborne experiments need to be conducted to provide accurate ground-based or airborne data for the validation of OMS SO_2 retrievals.

- **Response to comment "You refer to Section 5.2 for AMF and error details, but this section primarily describes RTM runs under various settings without quantitative error estimates relevant to your retrieval. A more robust discussion of structural uncertainties is needed."**

We agree with the reviewer that quantitative error estimates of each individual error source contributing to the SCD retrieval uncertainty and AMF uncertainty should be provided, and that the final propagated uncertainty in the VCD retrieval should be quantified.

Therefore, in the revised manuscript, we have rewritten Section 5 (Error analysis). The section now has four main subsections (Sections 5.1–5.4), with Section 5.1 further divided into five sub-subsections and

Section 5.2 into eight sub-subsections to systematically address different error components. The revised Section 5 is organized as follows. First, the major error sources affecting the SCD retrieval are listed, and the quantitative uncertainty of the OMS SO2 SCD retrieval is provided. Second, the main error sources influencing the AMF are analysed, and the AMF uncertainty associated with each error component is quantitatively estimated. Third, the residual errors after background offset correction are evaluated. Finally, based on the above results, overall quantitative estimates of the uncertainty of OMS SO_2 retrieval are presented.

Due to the large amount of newly added content and figures, please kindly refer the reviewer to the revised Section 5 (Error analysis) in the manuscript.

7. **Comment:** Section 5: I disagree with treating DOAS and AMF runs under different settings as an error analysis. The final SO_2 VCD product should be analyzed for uncertainty propagation. Figures 20-22 focus only on clear-sky conditions; what about cloud-related errors? Where is the σ_SO_2 analysis for OMS VCDs? Showing only sensitivity to inputs does not address true retrieval uncertainty. I recommend shortening Section 5 (also suggested by reviewer l) to focus specifically on the OMS SO_2 uncertainty, rather than on running the software (DOAS/RTM) under different settings.

Response: We thank the reviewer for these valuable comments. For clarity, we divide these comments into three parts and address them separately below.

(1) Response to "Section 5: I disagree with treating DOAS and AMF runs under different settings as an error analysis. The final SO_2 VCD product should be analyzed for uncertainty propagation", and "Showing only sensitivity to inputs does not address true retrieval uncertainty. I recommend shortening Section 5 (also suggested by reviewer l) to focus specifically on the OMS SO_2 uncertainty, rather than on running the software (DOAS/RTM) under different settings."

We agree with these comments. A more robust discussion of uncertainties is provided in Section 5 of the revised manuscript. Quantitative error estimates of each individual error source contributing to the SCD retrieval uncertainty and AMF uncertainty are now presented, and the final propagated uncertainty in the OMS SO_2 VCD retrieval is derived. To avoid redundancy, we refer the reviewer to our detailed response to Comment 6 and to Section 5 of the revised manuscript.

(2) Response to "Figures 20-22 focus only on clear-sky conditions; what about cloud-related errors?"

Due to the lack of synchronized and reliable OMS cloud data, most of the results and figures presented in this study are based on clear-sky conditions. The influence of clouds on AMF variability and associated

uncertainties has been investigated in previous studies, such as Lee et al. (2009). Some key findings from that study are quoted below:

> *"The clear-sky AMF error ranges from 15 to 30% over land and <15% over ocean. The cloudy-sky AMF error is 80– 160% over polluted regions and less elsewhere."*
>
> *"The error due to cloud pressure ranges from <10% over ocean to >100% over land."*
>
> *"The sensitivity of the AMF to cloud pressure is high when the cloud is collocated with high SO_2 mixing ratios, such as over China."*
>
> *"for polluted scenes the AMF error rapidly increases from 21% for cloud-free conditions to 245% for completely cloudy, reflecting the error in the correction for SO_2 obscuration by clouds."*

(3) Response to "Where is the σ_SO_2 analysis for OMS VCDs?"

The quantitative uncertainty (σ_SO_2) of OMS SO_2 VCD is now presented in Section 5.4 of the revised manuscript. This subsection describes the uncertainty propagation methodology and provides the final quantitative estimates of the OMS SO_2 VCD uncertainty.

For brevity, please kindly refer the reviewer to Section 5.4 of the revised manuscript.

8. **Comment:** Line 38: Please correct — not all satellites provide a global view; only low-Earth orbit (LEO) instruments offer near-global coverage.

   Response: Thank the reviewer for pointing this out. In the revised manuscript, the relevant text has been corrected at Line 50 as follows (shown in red):

   Low-Earth-orbit (LEO) satellite remote sensing offers the advantages of near-global coverage, short-term periodic observation capabilities, and continuous spatial coverage.

   In addition, we have carefully reviewed all occurrences of the term "global" throughout the manuscript to ensure that no similar mistake remain.

9. **Comment:** Lines 75–80: The description of the "spectral dimension to track dimension pixel" is somewhat confusing. Does this choice also affect the spatial resolution and is such an approach typical for other trace gas retrievals as well? If so, please elaborate. Otherwise, you may focus only on the VIS band for clarity.

   Response: Thank the reviewer for this comment and sorry for the lack of clarity in our previous

description. The "spectral dimension to track dimension pixel" refers to the onboard spatial binning strategy applied at the OMS L1 processing stage, which consequently affects the spatial resolution of all OMS L2 trace gas products (e.g., O_3, NO_2, SO_2, HCHO).

To clarify this point, we have revised and expanded the related description in the revised manuscript, replacing the previous text (in blue font) with the revised text (in red font) as shown below.

OMS-N operates using a push-broom observation technique to obtain daily global measurements, with a wide Field of View (FOV) of 112°, covering three spectral bands: UV1 (250-300 nm), UV2 (300-320 nm), and VIS (307-493 nm). To enhance the signal-to-noise ratio (SNR) of the original detector rows, sets of 16 pixels are averaged to yield 58 spatial rows in the UV1 band, and four pixels are averaged to acquire 238 spatial rows in the UV2 and VIS bands, respectively (Wang et al., 2024).

OMS-N operates using a push-broom observation technique to obtain daily global measurements, with a wide Field of View (FOV) of 112°. It incorporates two imaging grating spectrometers covering the UV (250-320 nm) and VIS (307-493 nm) bands, where the UV measurements are divided into the UV1 (250-300 nm) and UV2 (300-320 nm) sub-bands. Each spectrometer uses a 1024 × 1024 pixel imaging array, with one dimension recording spatial information along the slit and the other recording spectral information. To enhance the signal-to-noise ratio (SNR) of the original detector rows, OMS L1 applied an onboard spatial binning strategy: sets of 16 pixels were averaged to yield 58 cross-track spatial rows in the UV1 band, and 4 pixels were averaged to produce 238 cross-track spatial rows in the UV2 and VIS bands, respectively. The remaining spatial rows were reserved for calibration purposes.

10. Comment: Equatorial overpass time (10:00 AM): Please clarify whether this refers to local time or UTC. Although it may be obvious to some, this clarification would benefit many readers.

Response: Thank the reviewer for pointing this out. The equatorial overpass time refers to local time. In the revised manuscript, we have corrected this by replacing "10:00 AM" with "10:00 AM (local time)" in Table 1.

11. Comment: Section 3: Please specify that the VIS band in the 312–326 nm region is chosen (line 89).

Response: Thank the reviewer for this comment. Strictly speaking, the 312–326 nm spectral region does not belong to the visible (VIS) band; however, in the OMS L1 data product, channels covering 307–493 nm are collectively referred to as the VIS band. To avoid confusion, this statement has been removed in the revised manuscript, as also addressed in our response to Comment 3.

12. Comment: When listing retrieval steps in Section 3, please remove words such as "Firstly," "Secondly,"

etc., if numbers are already provided.

Response: Thanks for this comment. As mentioned in the response to Comment 3, in order to achieve more concise expressions, we have removed and shortened redundant descriptions of the OMS SO_2 retrieval steps. Specifically, the previously listed detailed retrieval steps (Points 1–8) have been condensed into the following summary (in red font) while still retaining the key procedures of the OMS SO_2 DOAS retrieval:

The SO_2 retrieval from FY-3F/OMS involves radiance normalization, spectral soft calibration, convolution of SO_2 and O_3 cross-sections and Ring spectrum with the OMS-N Instrument Spectral Response Function (ISRF), DOAS fitting to obtain SO_2 SCD, AMF conversion to vertical column density (VCD), and background offset correction to reduce striping and across-track asymmetries.

13. Comment: If these are the first OMS SO_2 retrievals, please clarify what "initial" means, is this the first-ever retrieval, or an early version used for calibration/validation prior to final algorithm release? (Line 17 and line 96)

Response: We apologize for not explaining this clearly in the manuscript. The term "initial" used at Lines 17 and 96 refers to the preliminary SO_2 retrieval results obtained directly from the DOAS fitting, which are not yet corrected for background offsets and still contain substantial systematic striping errors. After applying the background offset correction, these systematic biases present in the initial DOAS results are largely removed.

To avoid ambiguity, the term "initial" has been replaced with "raw" in the revised manuscript.

14. Comment: Line 97-99: Please explain why no cloud information (e.g., cloud fraction or cloud height) is retrieved here. Cloud properties can strongly influence both spectra and AMF values, and correct cloud filtering is essential. How were cloudy pixels handled in your retrieval? Please provide stronger justification for the statement.

Response: Thank the reviewer for this comment.

We agree that cloud properties can strongly influence both the measured spectra and AMF values, and the appropriate cloud filtering is essential for accurate SO_2 retrievals.

At the time of writing, the OMS cloud product was still under development, and synchronized and reliable cloud data were not yet available. The use of inaccurate cloud information would introduce even larger uncertainties into the final SO_2 retrievals. In addition, employing cloud products from other satellite instruments could also lead to large errors due to differences in spatial resolution, spectral characteristics,

and overpass time. Developing an independent cloud retrieval for OMS would require considerable time and technical effort. Therefore, for this first presentation of OMS SO_2 retrieval results, we focused primarily on clear-sky conditions.

In future work, once improved and reliable OMS cloud products become available, we will incorporate cloud information to better account for cloud-related effects and to quantitatively assess the associated uncertainties in OMS SO_2 retrievals.

15. Comment: Line 160: It would be helpful to include the expected precision of OMS SO_2 columns (either pre-launch or post-launch) to explain the occurrence of negative values.

Response: Thank the reviewer for this suggestion.

We have added the OMS L1 calibration requirements before launch in Table 4 of the revised manuscript. Based on pre-launch laboratory characterizations of the OMS instrument, the expected uncertainty of OMS SO_2 vertical column is on the order of less than 30%.

Regarding the occurrence of negative SO_2 values, this phenomenon is not unique to OMS. Negative values commonly appear in SO_2 retrievals from many satellite instruments, such as OMI, GOME-2, and TROPOMI, and small negative values often indicate very low SO_2 concentrations in clean regions (Theys et al., 2013; Fioletov et al., 2020). Over oceanic areas, where SO_2 concentrations are low, the retrieved values tend to fluctuate around zero due to measurement noise and fitting errors, resulting in frequent negative values. In addition, the background offset correction process may inevitably lead to slight overcorrection or undercorrection, which is also a major contributor to the occurrence of negative values.

16. Comment: Line 303: The statement "the OMS SO_2 retrievals tend to be systematically overestimated or underestimated over the whole orbit" — relative to what reference? Please specify.

Response: We apologize for the unclear description in the manuscript. This statement was inappropriate, and it has been removed in the revised manuscript.

17. Comment: Figure 8g: The interpretation is unclear without knowing the precision of OMS SO_2. Are the negative values due to limited precision? Also clarify whether the SO_2 columns in Section 4.1 represent SCDs or VCDs. Also, please check for consistency, you've used the term SO_2 column to refer to SCDs in some places as well.

Response: Thank the reviewer for these comments.

First, the overall precision of OMS SO_2 over clean oceanic regions were added in the revised manuscript

(Line 341), with an estimated precision of approximately 0.15 DU.

Regarding the occurrence of negative SO_2 values, this phenomenon is not unique to OMS. Negative values commonly appear in SO_2 retrievals from many satellite instruments, such as OMI, GOME-2, and TROPOMI, and small negative values often indicate very low SO_2 concentrations in clean regions (Theys et al., 2013; Fioletov et al., 2020). Over oceanic areas, where SO_2 concentrations are low, the retrieved values tend to fluctuate around zero due to measurement noise and fitting errors, resulting in frequent negative values. In addition, the background offset correction process may inevitably lead to slight overcorrection or undercorrection, which is also a major contributor to the occurrence of negative values.

With respect to the use of SCDs and VCDs, we have carefully checked the revised manuscript for consistency. Unless explicitly stated as SCD, all SO_2 columns in the revised manuscript now refer to VCD.

18. Comment: Line 465: "It is worth noting that the retrieval errors for both OMS and TROPOMI are relatively large at the edges of the orbit." While higher σ values are seen in Fig. 9h/i, these may also result from fewer pixels (data gaps) or TROPOMI's larger pixel size (roughly double that at nadir). Please clarify.

Response: Thanks for this comment. The manuscript has been revised accordingly. The following text (shown in red font) has replaced the original sentence.

It is worth noting that the retrieval errors for both OMS and TROPOMI are relatively large at the edges of the orbit, which is likely due to fewer valid pixels in these regions, resulting in larger standard deviations.

19. Comment: Figure 7: Please number each selected region and refer to those numbers in the text where discussed.

Response: Thank the reviewer for this suggestion. We have revised the figure as shown below. We have also updated the manuscript to refer to these region numbers where they are discussed. Please refer to the revised manuscript for details.

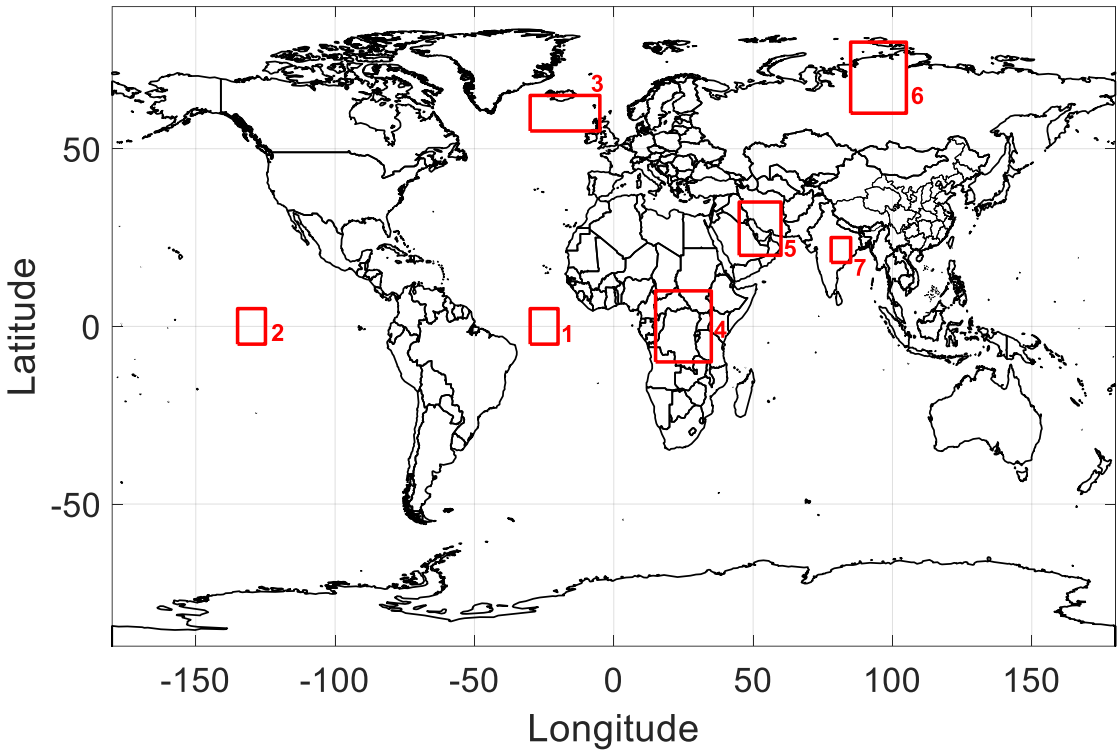

Regions selected for the comparison of OMS and TROPOMI SO_2 columns. Regions 1 and 2 represent clean oceanic areas, regions 3 and 4 correspond to volcanic eruption areas, and regions 5–7 represent anthropogenic emission areas.

20. Comment: Figure 6: These are SCD values; please clarify whether Figures 10–11 and others show SCDs or VCDs.

Response: Thanks for this comment. We apologize for not clearly specifying this. In the revised manuscript, unless explicitly stated as SCD, all SO_2 columns now refer to VCDs.

21. Comment: The repeated statement "We used all pixels from the TROPOMI DOAS SO_2 product instead of applying QA > 0.5", is concerning. The QA filter is crucial for high-quality data, as high SO_2 values can appear in cloudy scenes. How was cloud contamination accounted for if the QA filter was removed?

Response: Thank the reviewer for pointing this out. We agree that the TROPOMI QA filter play an essential role in ensuring the reliability of the TROPOMI SO_2 retrievals, particularly by reducing cloud contamination.

However, the QA filter was not applied in Sections 4.2 and 4.3. This is because the TROPOMI QA flag is not always reliable in special situations such as volcanic eruptions or bright surfaces (snow/ice). For volcanic eruption cases, we found that applying the QA > 0.5 filter to the TROPOMI DOAS SO_2 product often removes a large portion of high SO_2 pixels. A similar issue is also observed for strong anthropogenic emission cases, although to a lesser extent.

To illustrate this clearly, we compared TROPOMI DOAS SO_2 with and without the QA > 0.5 filter and also included the TROPOMI COBRA L3 product (already filtered with QA > 0.5) as a reference. These comparison figures are provided at the end of this response. From these comparisons, our main findings are as follows:

(1) Volcanic eruption: Volcanic SO_2 plumes often rise to higher altitudes where they remain detectable even in the presence of clouds. However, the TROPOMI QA flags often misclassify plume pixels as low quality. Consequently, applying the QA > 0.5 filter result in that a large portion of high SO_2 pixels around volcanic regions were identified as invalid pixels, making meaningful comparison with OMS SO_2 difficult.

(2) Anthropogenic emission: The QA > 0.5 filter also removes some high SO_2 pixels, though less severely than in volcanic cases.

(3) In addition, in regions without volcanic or strong anthropogenic emissions, the pixels removed by the QA filter do not exhibit anomalously high values.

Therefore, for the comparison between OMS and TROPOMI in Sections 4.2 and 4.3, we used all TROPOMI DOAS pixels rather than applying QA > 0.5.

We acknowledge that cloud contamination cannot be neglected and that selecting clear-sky pixels is still crucial whenever possible. In this study, to minimize the influence of cloud-contaminated pixels, we adopted the following strategy in the manuscript:

(1) Clean oceanic regions (Section 4.1): we applied the QA > 0.5 filter to the TROPOMI DOAS SO_2 data because clouds strongly affect low SO_2 regions and accurate statistics are required for comparison in clean oceanic regions.

(2) Anthropogenic emission regions (Section 4.3): Monitoring boundary-layer SO_2 from anthropogenic sources is highly susceptible to cloud interference. To minimum limit the cloud contamination, MODIS true-color images were used to select orbits with minimal cloud cover.

We hope that the above responses provide a satisfactory answer to the reviewer's comment. We agree that neglecting cloud and aerosol effects may introduce non-negligible biases, especially for PBL SO_2 retrievals. Once accurate OMS cloud products become available in the future, we will incorporate cloud-screened OMS SO_2 results to support more application studies.

Cases of Volcanic Eruptions

(top to bottom: Sundhnúkur volcano on 2024-08-23, and Nyamuragira volcano on 2024-11-03, 2024-11-08, and 2024-11-15).

TROPOMI DOAS SO_2 with QA>0.5

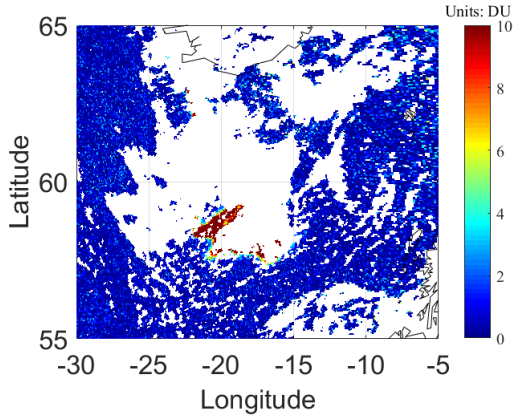

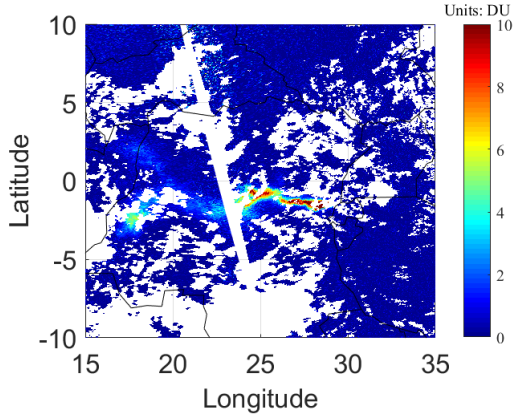

TROPOMI DOAS SO_2 without QA filtering

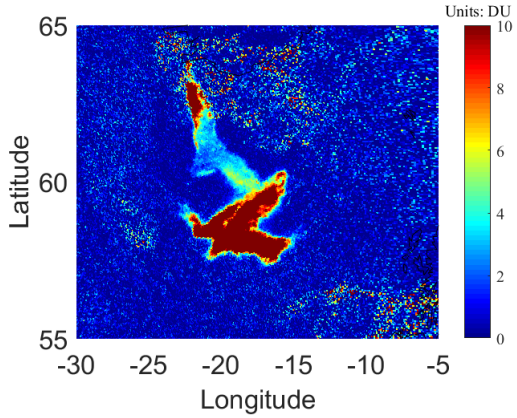

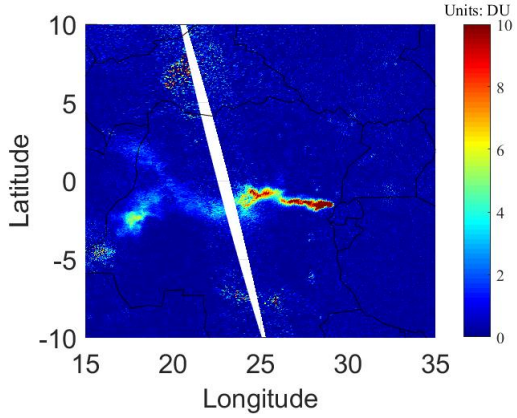

TROPOMI COBRA L3 grid 7km SO_2

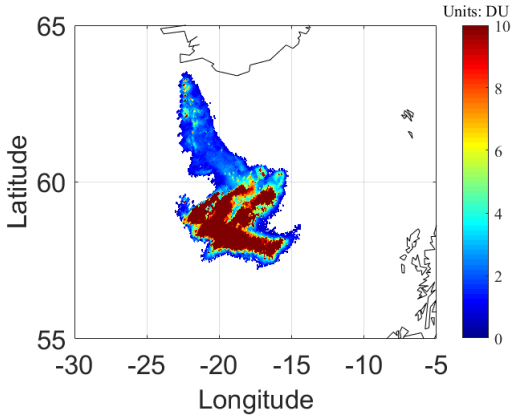

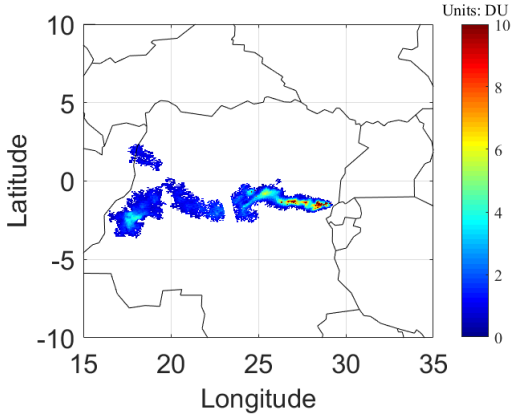

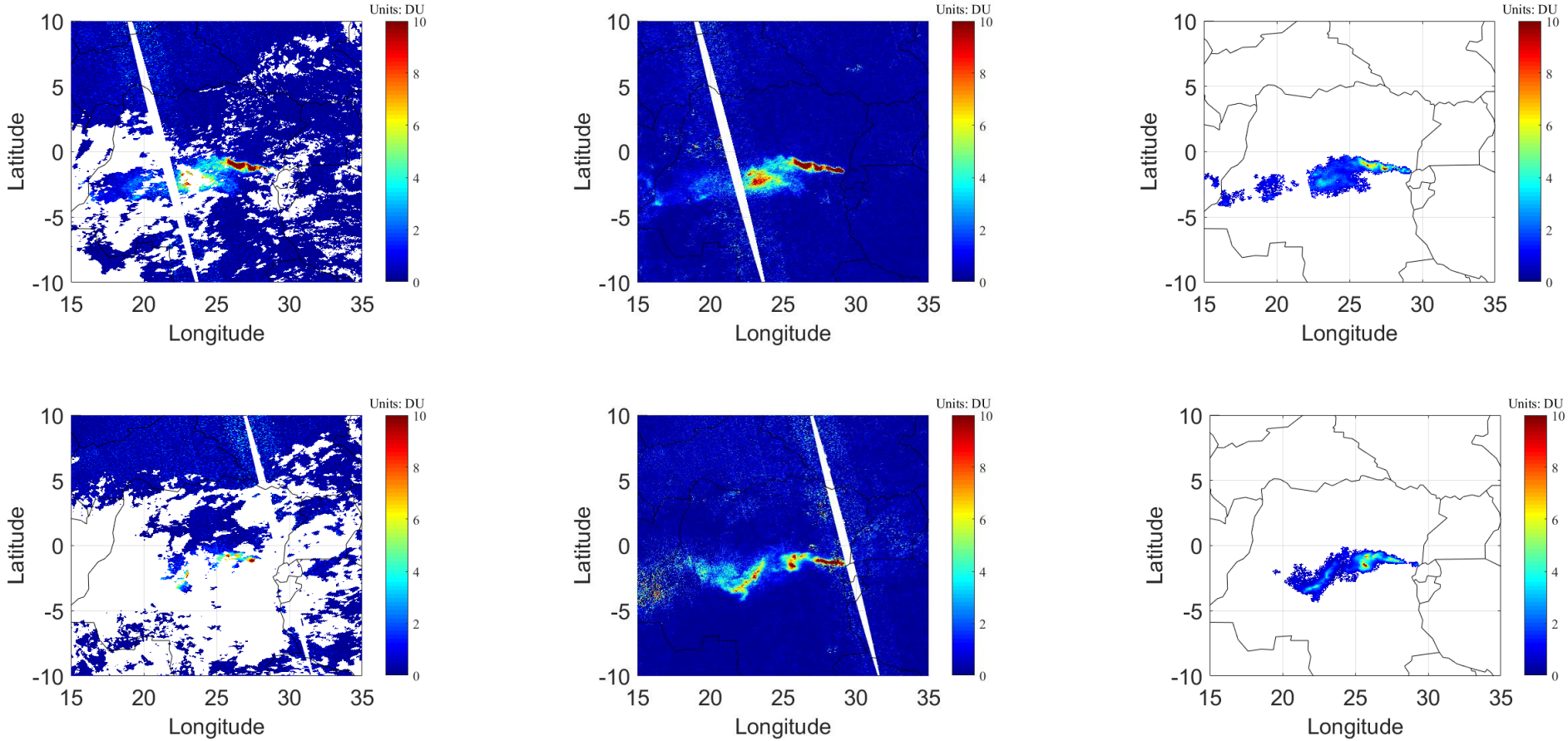
Units: DU
Latitude
Longitude
10
5
0
-5
-10
15
20
25
30
35
0
2
4
6
8
10

Cases of Anthropogenic Emissions

(top to bottom: Persian Gulf—2024-08-23; Persian Gulf—2024-11-12; Norilsk—2024-05-16 (TROPOMI Orbit 1); Norilsk—2024-05-16 (TROPOMI Orbit 2); Eastern India—2024-11-04; Eastern India—2024-11-05; Eastern India—2024-11-09).

TROPOMI DOAS SO_2 with QA>0.5

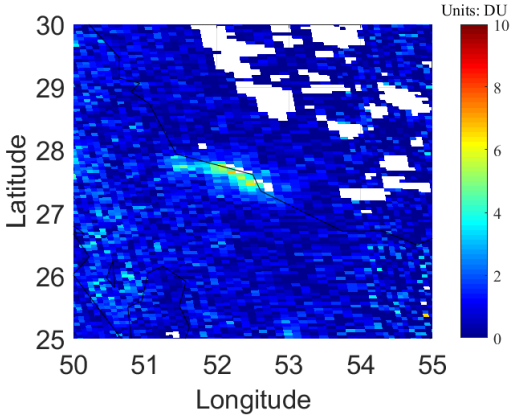

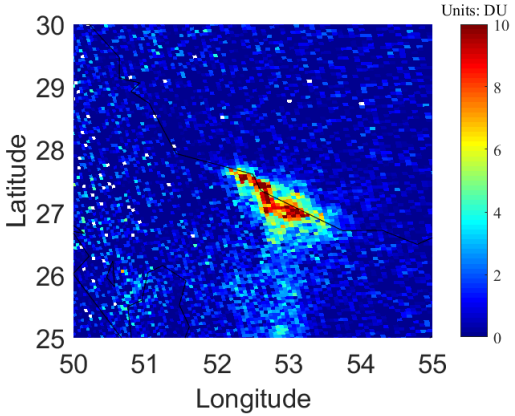

TROPOMI DOAS SO_2 without QA filtering

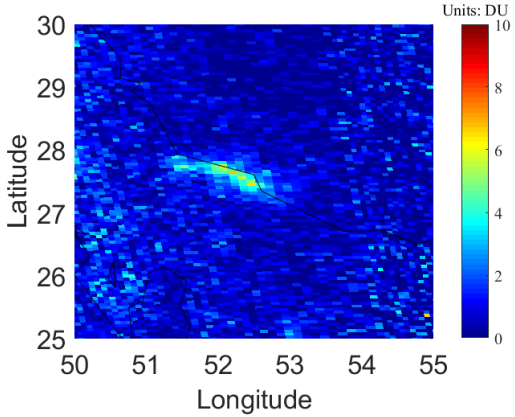

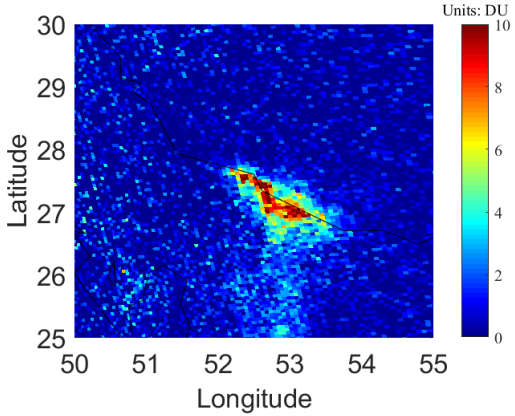

TROPOMI COBRA L3 grid PBL SO_2

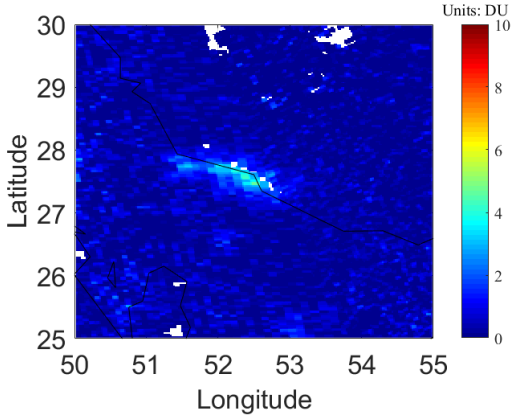

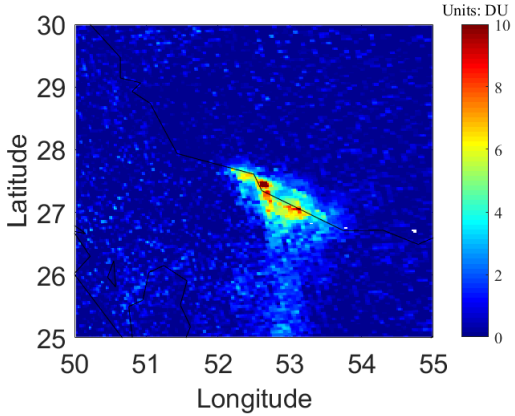

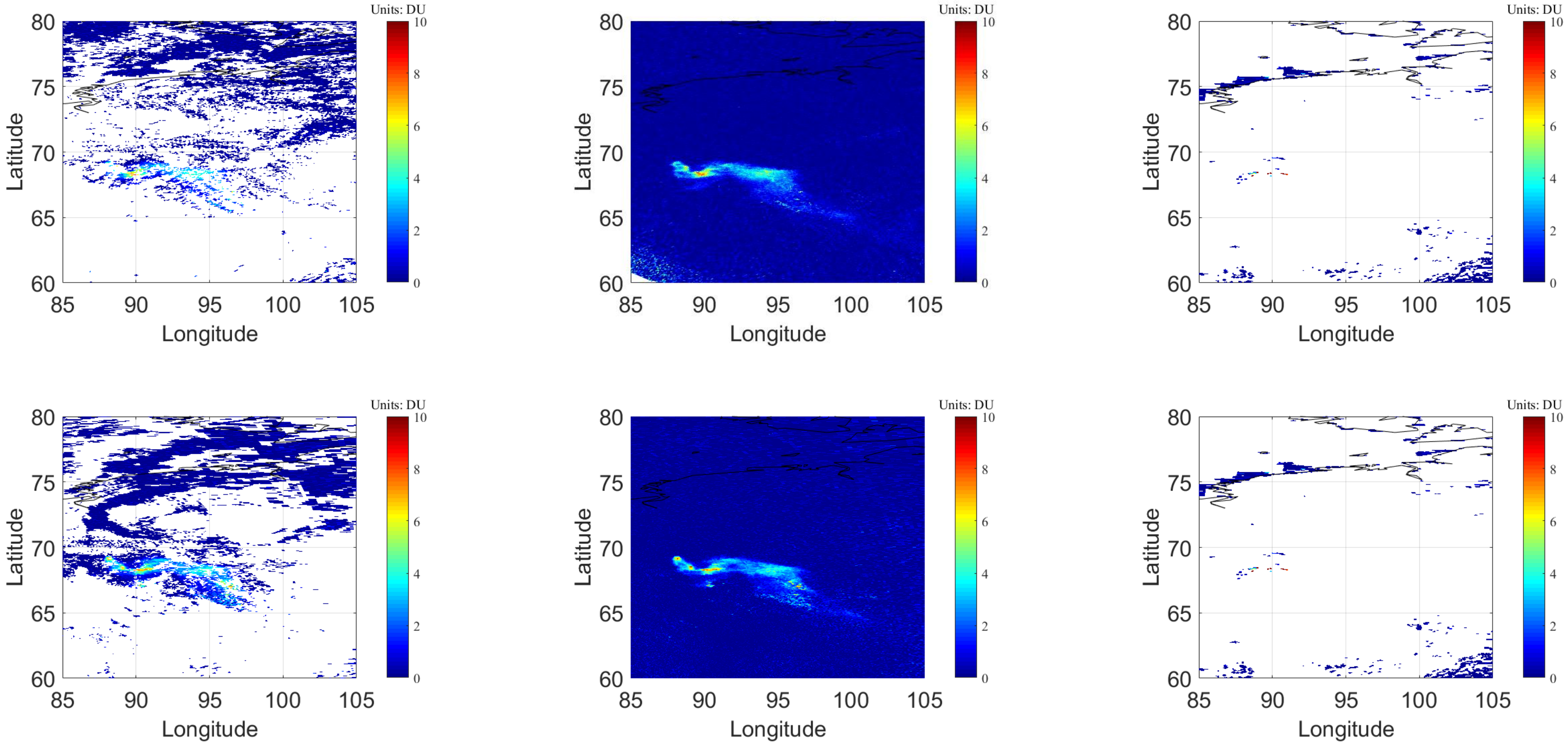
Units: DU
Latitude
Longitude

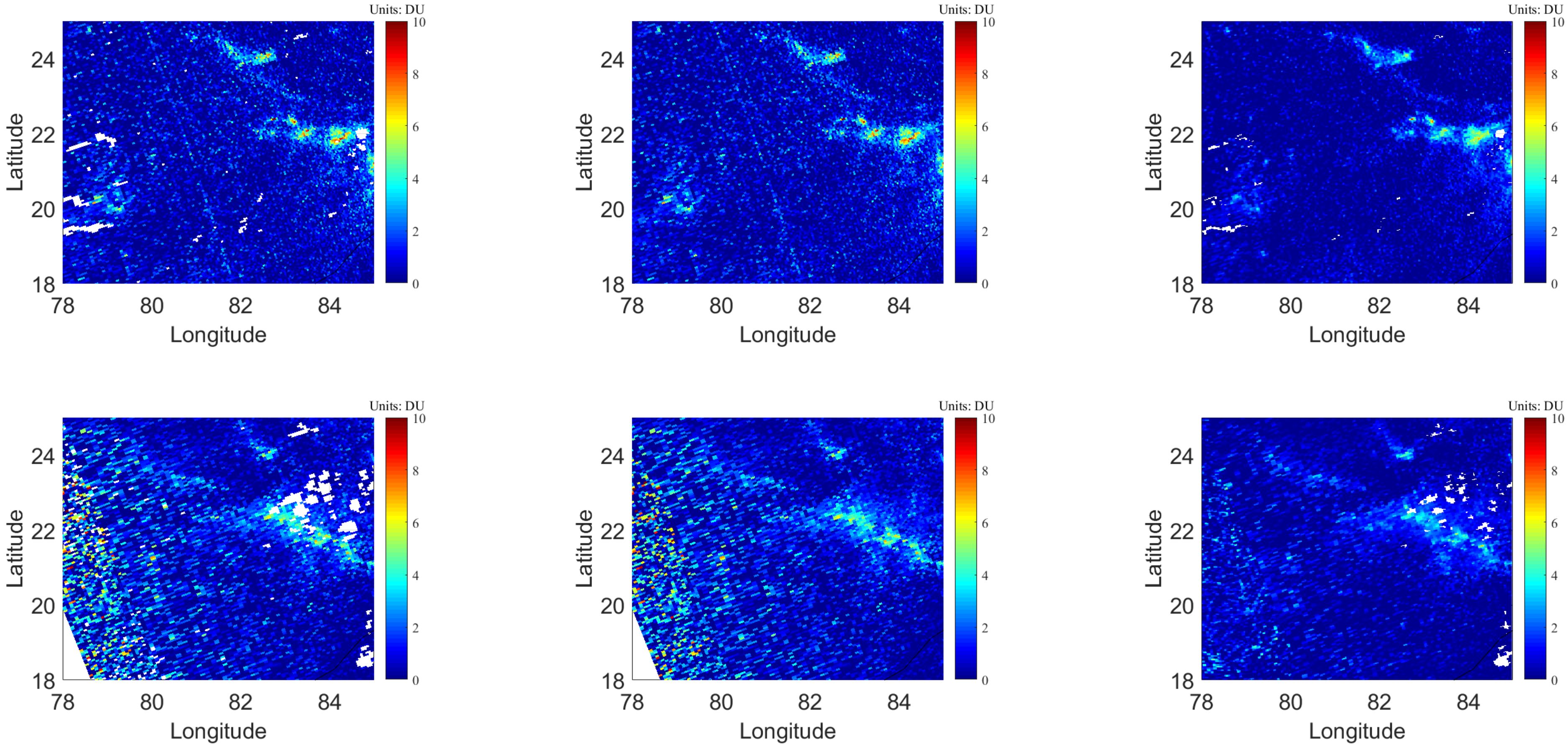

Units: DU
10
8
6
4
2
0
Latitude
24
22
20
18
78
80
82
84
Longitude

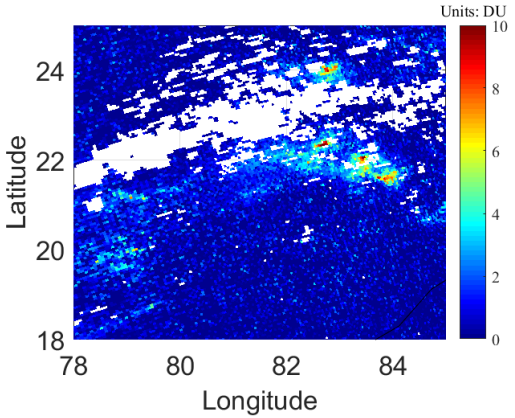
Units: DU
10
8
6
4
2
0
Latitude
24
22
20
18
78
80
82
84
Longitude

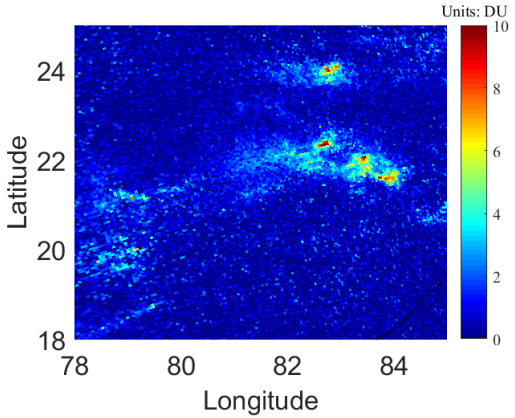
Units: DU
10
8
6
4
2
0
Latitude
24
22
20
18
78
80
82
84
Longitude

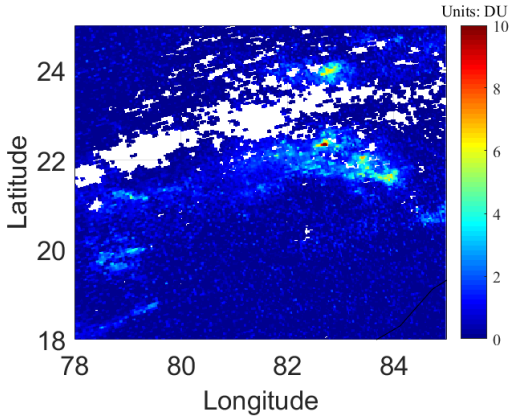
Units: DU
10
8
6
4
2
0
Latitude
24
22
20
18
78
80
82
84
Longitude

22. Comment: Figures 12–18: These show the great potential of OMS SO_2 data for identifying emission sources. However, as this is the first publication on the product, presenting more days of quality-controlled, averaged data (e.g., over volcanic or anthropogenic periods) would strengthen the conclusions.

Response: Thank the reviewer for this valuable suggestion. Following this recommendation, we have added OMS SO_2 retrieval results for additional orbits and days in Sections 4.2 and 4.3 to better demonstrate the capability of the OMS product in identifying emission sources.

For example, in Section 4.3, the OMS SO_2 retrievals over the Persian Gulf have been extended from the previous two days to seven days (23 August 2024 and 3, 4, 7, 8, 12, and 14 November 2024). The OMS SO_2 retrievals over Eastern India have been increased from three days to four days (4, 5, 8, and 9 November 2024). In Section 4.2, the OMS SO_2 retrievals over the Nyamuragira volcano have been expanded from three days to four days (3, 8, 13, and 15 November 2024). Due to the large number of newly added figures, we kindly refer the reviewer to the revised manuscript for details.

In addition, we have plotted additional OMS SO_2 results over volcanic activity in Ethiopia in November 2025 (see Supplement-3, which is included at the end of this document). It should note that at the time of writing, the corresponding synchronized AMF calculations had not yet been fully processed; therefore, the results shown in Supplement-3 are OMS SO_2 SCDs.

23. Comment: Line 885: This is not a "box-AMF"; it represents scattering weights, which are then combined with an a priori profile to construct the AMF. Please correct.

Response: Thanks for this comment.

The content of Line 885 in the previous version of the manuscript is shown below (italicized):

"Additionally, for SO_2 retrievals from high spatial resolution satellite observations, it is often necessary to build a Box-AMF lookup table (LUT) by using a radiative transfer model that considers variables such as SZA, VZA, RAA, AS, HS, wavelength, O_3 column, and cloud cover."

After discussion with the coauthors and consultation with Dr. Alexey Rozanov, one of the SCIATRAN developers, our understanding of the relationship between box-AMFs, scattering weights, and weighting functions is as follows:

(1) Box-AMFs and scattering weights

In the European view of AMFs, the SCIATRAN model computes so-called box-AMFs (historically referred to as block-AMFs), which are defined as the air mass factor that a trace gas would have if it were present only in a given altitude layer and nowhere else. Under the assumption of optically thin absorption, the total AMF can be obtained by summing the box-AMFs weighted by the partial columns of the a priori vertical profile and normalizing by the total a priori column. This represents the commonly used European interpretation of AMFs.

(2) US terminology: scattering weights

In contrast, in the U.S., following the terminology of Palmer et al. (2001), the same quantity is typically referred to as scattering weights, which are combined with the unitless shape factor of the vertical profile to construct the AMF.

(3) Relation to weighting functions

In non-DOAS applications, a closely related concept is the radiance weighting function. When computed for radiance, this quantity can be readily converted to a box-AMF by division by the vertical optical depth of the absorber.

Based on this, we use SCIATRAN to calculate box-AMFs (i.e., scattering weights in U.S. terminology) under different input conditions and to construct a corresponding lookup table.

The terminology in the revised manuscript has been clarified accordingly. Specifically, the sentence in Line 885 has been revised as follows (in red font):

"Additionally, for SO_2 retrievals from high spatial resolution satellite observations, it is often necessary to build a Box-AMF (also referred to as scattering weights) lookup table

(LUT) by using a radiative transfer model that considers variables such as SZA, VZA, RAA, AS, HS, wavelength, O_3 column, and cloud cover."

24. Other revisions:

In addition to the revisions described above, we have made further minor modifications throughout the manuscript to improve clarity, consistency, and overall readability. Please refer to the tracked-changes version of the manuscript and the revised manuscript for detailed modifications.

Supplement-1

Employs geometric AMFs (hereafter referred to as AMFgeo) to convert OMS SO_2 SCDs to VCDs.

OMS AMFgeo (orbit 20240516_0516)

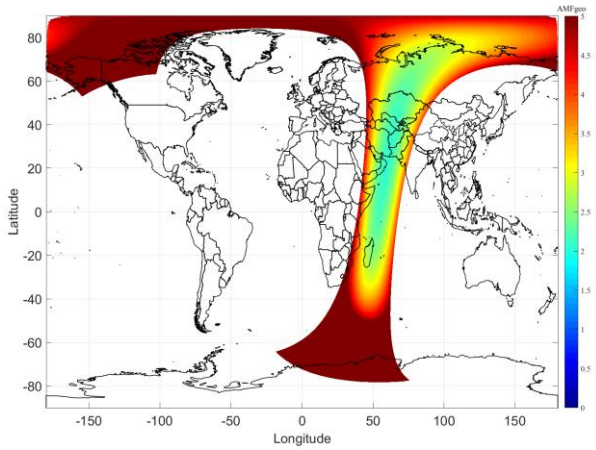

OMS AMFgeo (orbit 20240823_1217)

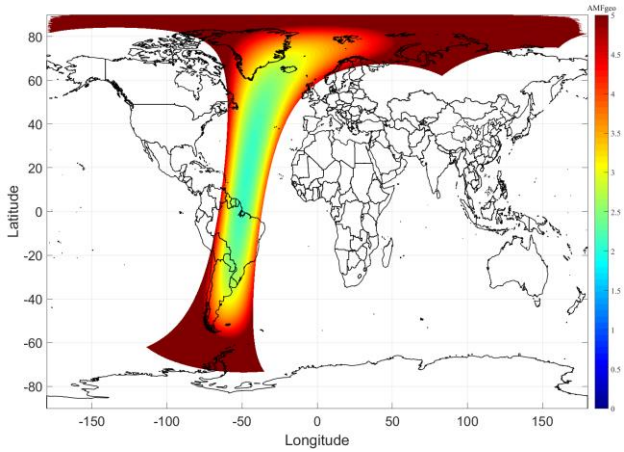

OMS AMFgeo (orbit 20241109_0401)

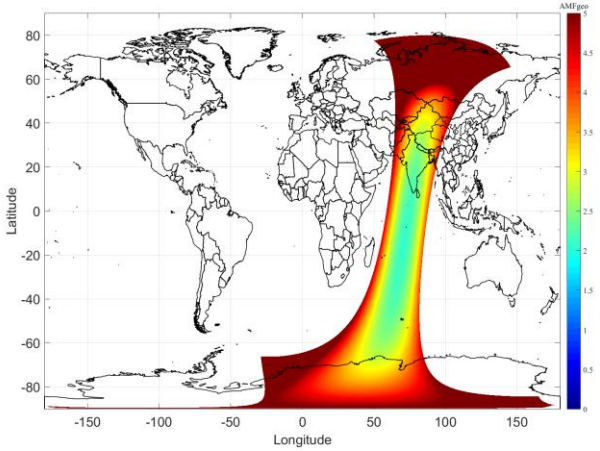

Region 1 (ocean area), 20240823

OMS SO_2 SCDs	OMS SO_2 VCDs using AMFgeo	TROPOMI DOAS SO_2 VCDs	TROPOMI COBRA PBL SO_2 VCDs
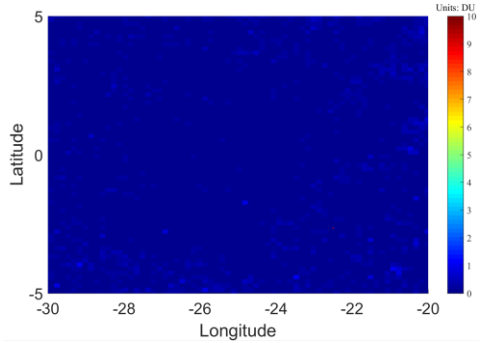	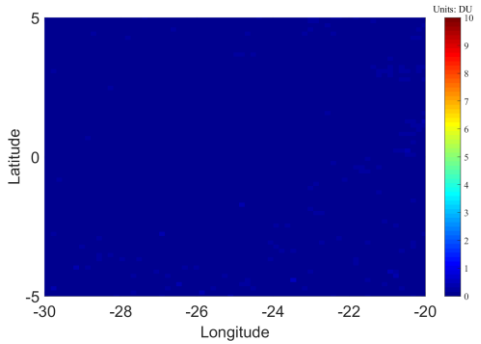	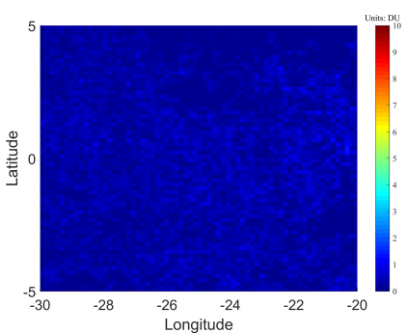	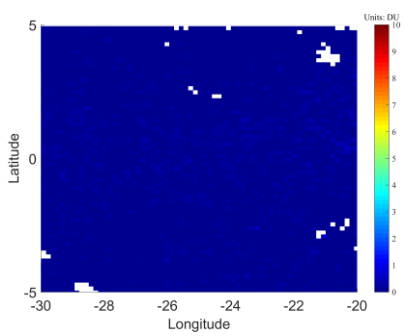
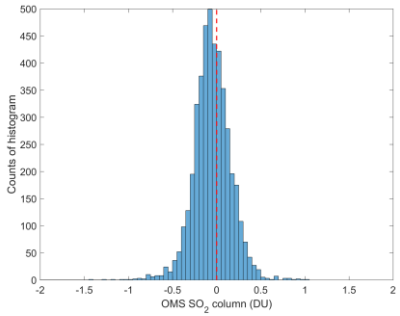	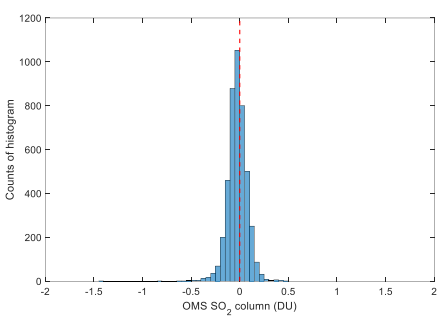	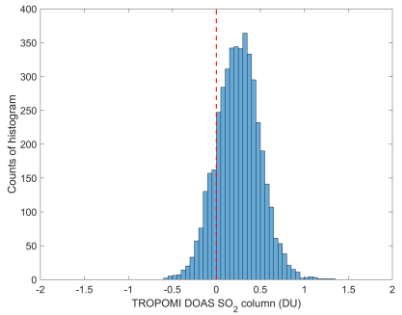	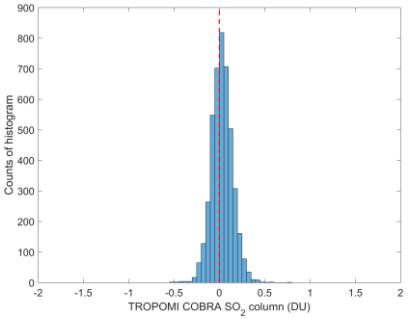
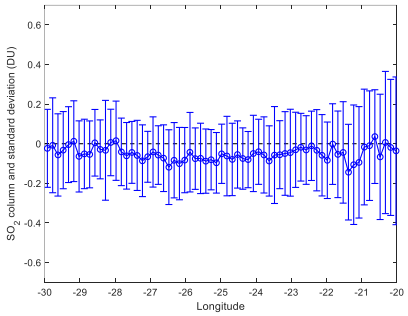	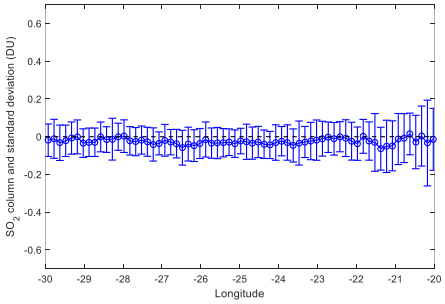	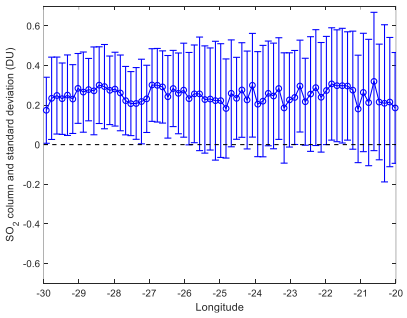	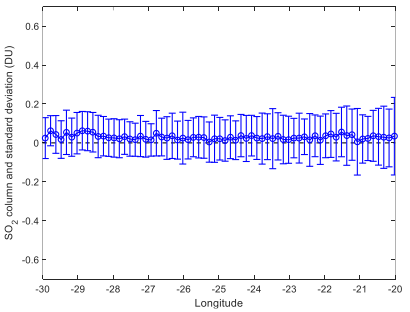

Region 1 (ocean area), 20241115

OMS SO_2 SCDs	OMS SO_2 VCDs using AMFgeo	TROPOMI DOAS SO_2 VCDs	TROPOMI COBRA PBL SO_2 VCDs
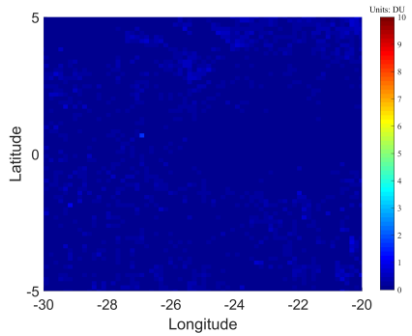	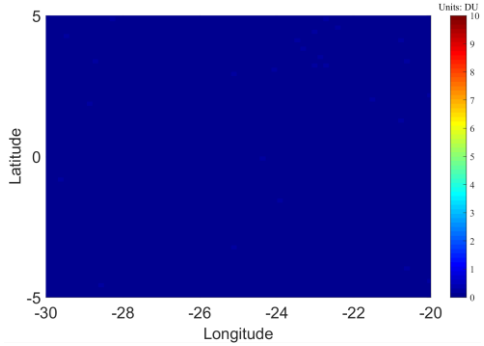	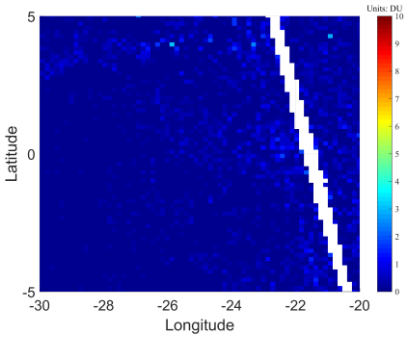	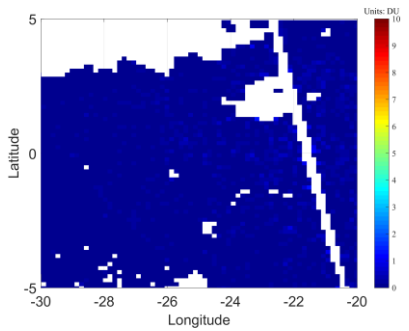
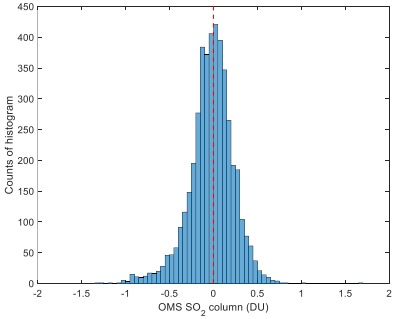	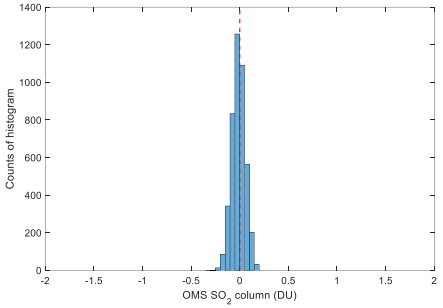	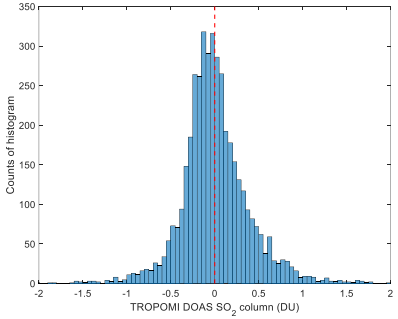	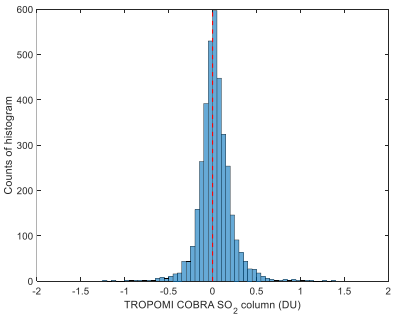
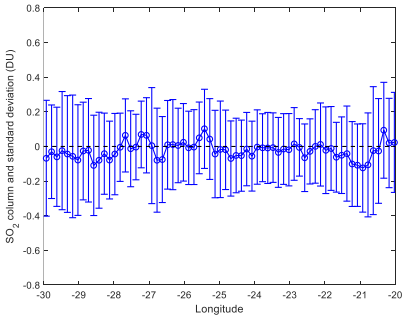	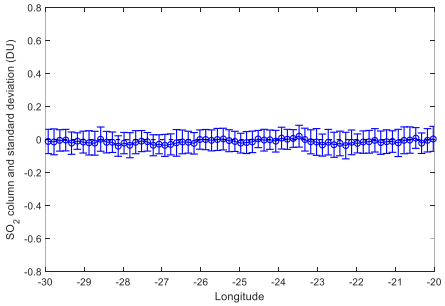	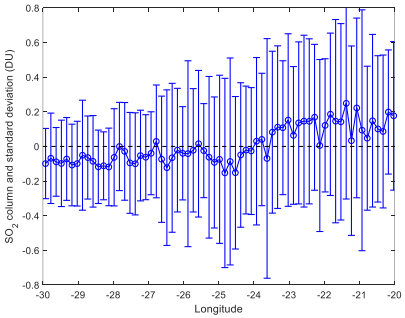	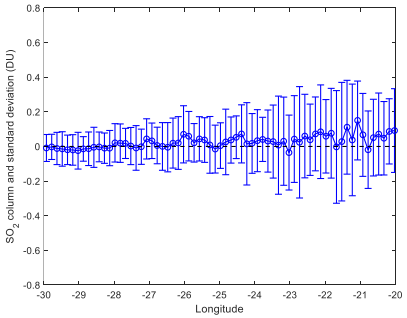

Region 2 (ocean area), 20240823

OMS SO_2 SCDs	OMS SO_2 VCDs using AMFgeo	TROPOMI DOAS SO_2 VCDs	TROPOMI COBRA PBL SO_2 VCDs
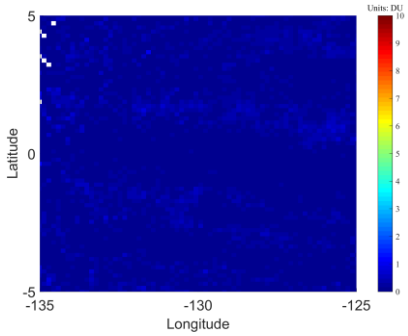	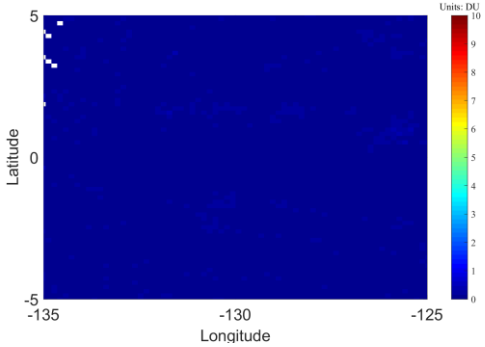	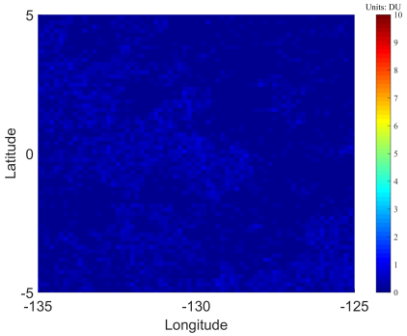	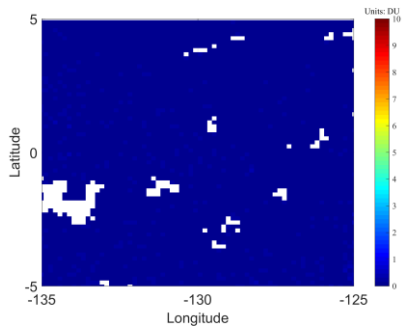
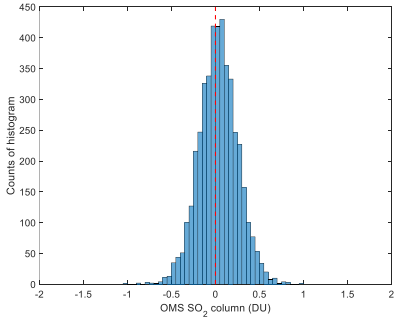	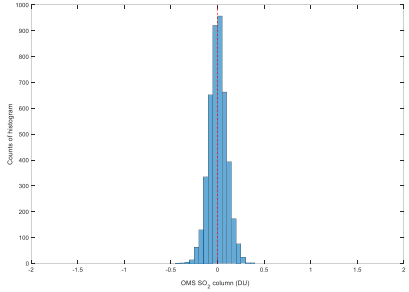	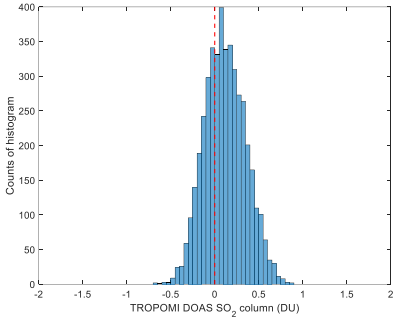	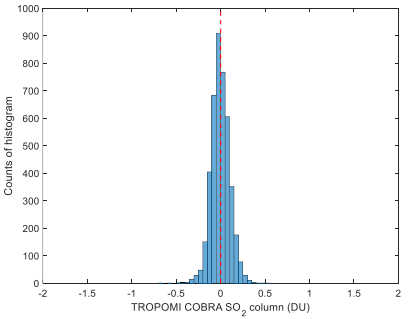
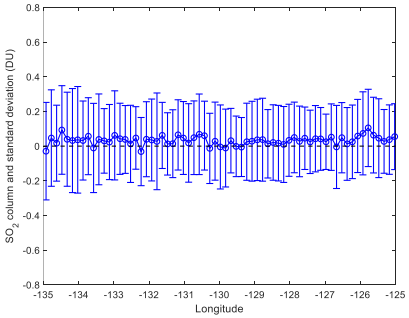	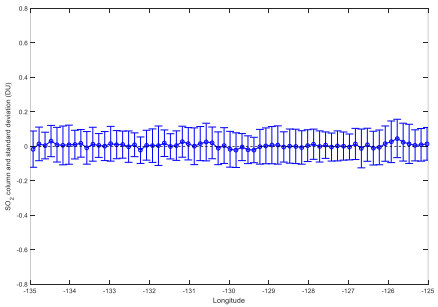	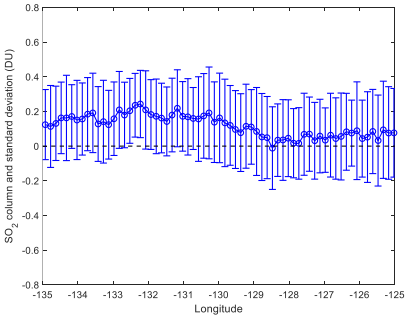	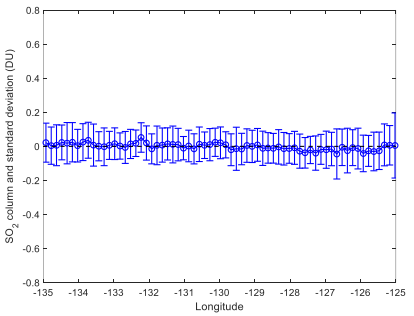

Region 2 (ocean area), 20241115

OMS SO_2 SCDs	OMS SO_2 VCDs using AMFgeo	TROPOMI DOAS SO_2 VCDs	TROPOMI COBRA PBL SO_2 VCDs
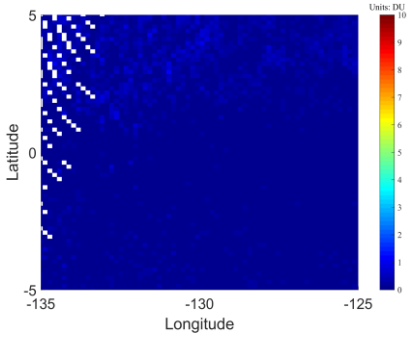	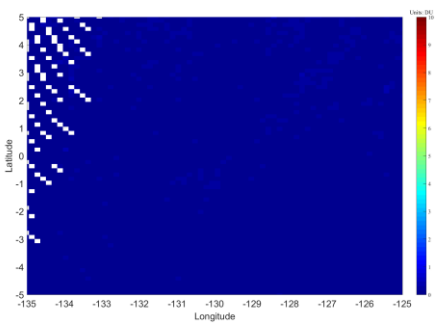	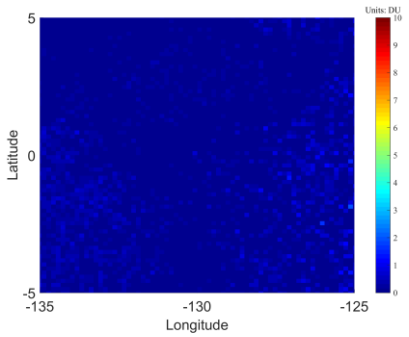	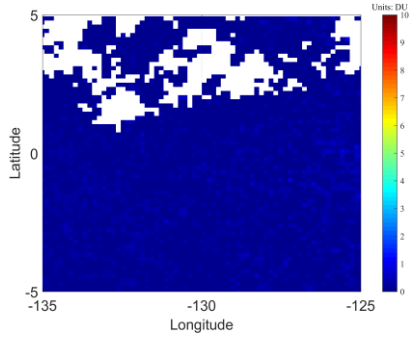
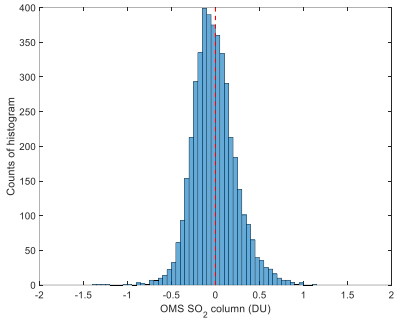	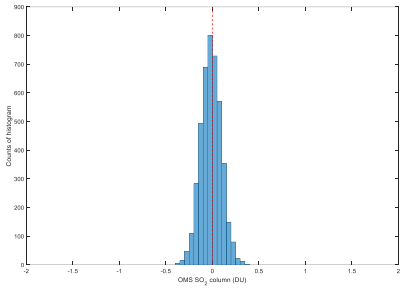	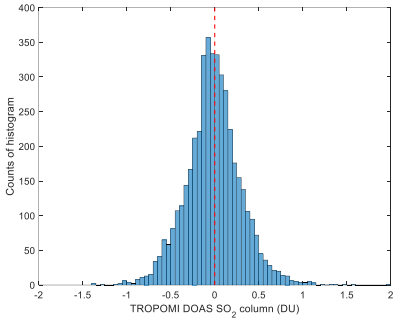	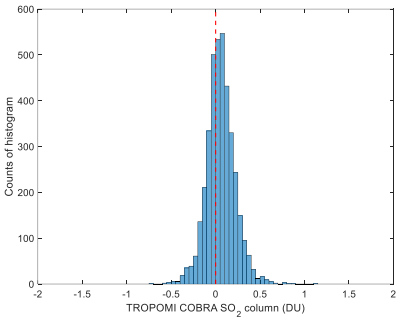
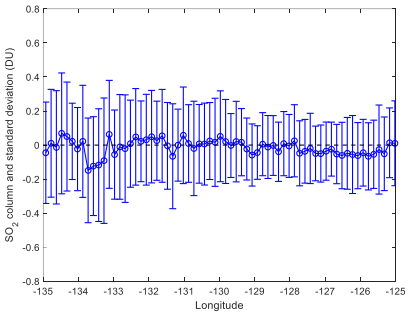	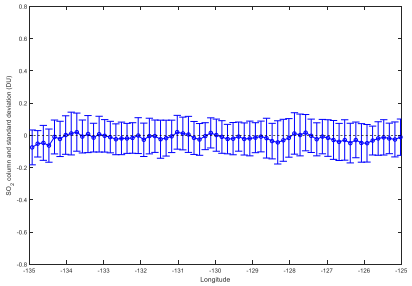	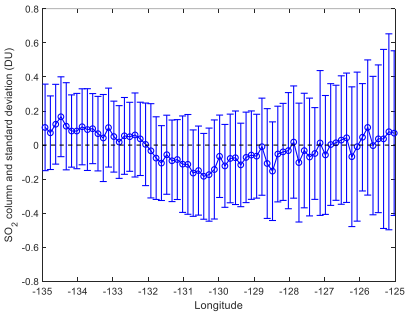	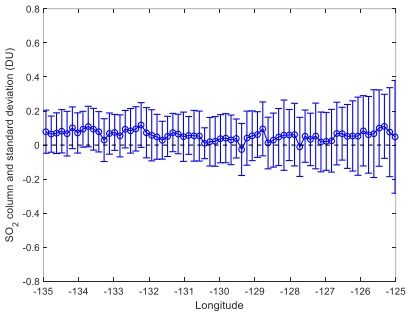

SO_2 retrievals over Sundhnúkur volcano on August 23, 2024.

OMS SO_2 SCDs

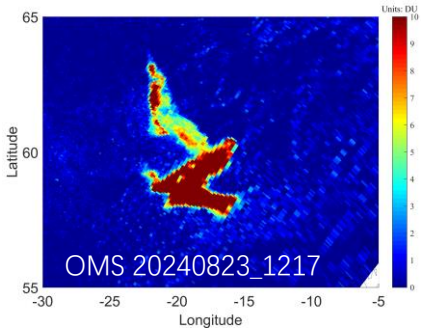

OMS SO_2 VCDs using AMFgeo

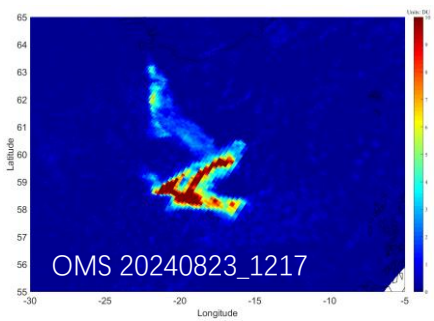

TROPOMI DOAS SO_2 VCDs

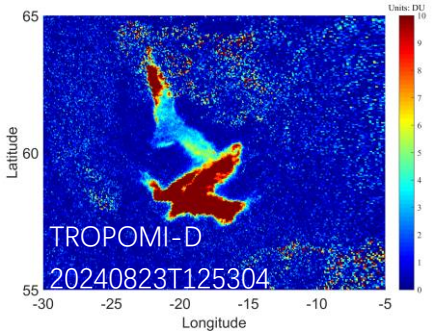

TROPOMI COBRA 7km SO_2 VCDs

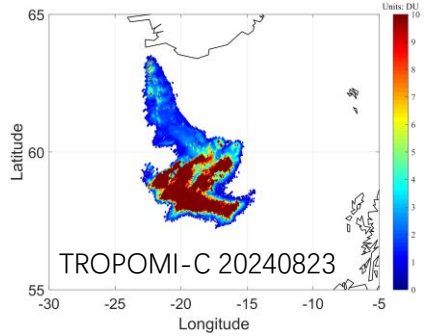

OMS AMFgeo

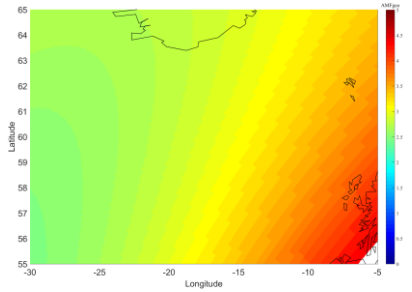

OMS SO_2 VCDs using AMFgeo Vs. TROPOMI DOAS SO_2 VCDs

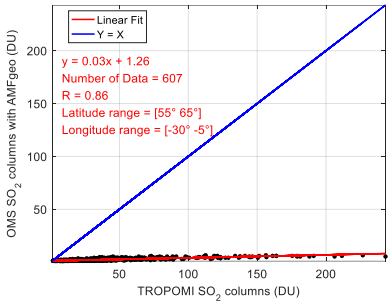

OMS SO_2 SCDs Vs. TROPOMI DOAS SO_2 VCDs

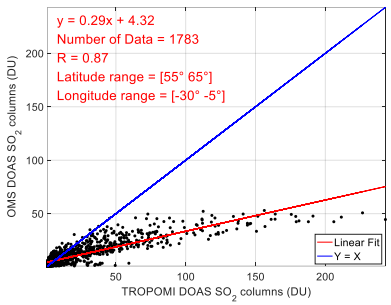

OMS SO_2 SCDs Vs. TROPOMI COBRA 7km SO_2 VCDs

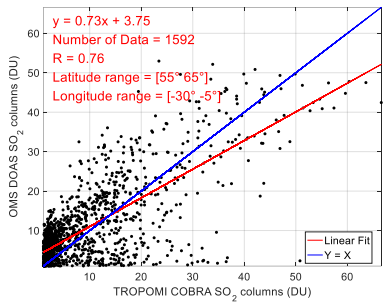

OMS SO_2 SCDs

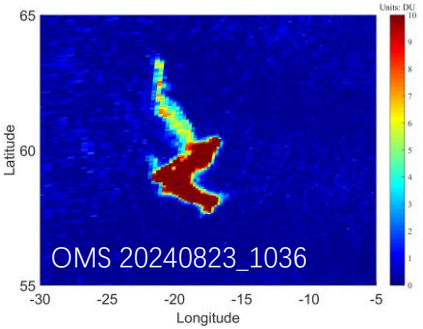

OMS SO_2 VCDs using AMFgeo

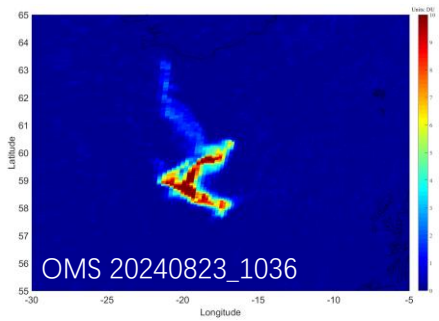

Figure: SO_2 retrievals of OMS and TROPOMI over Sundhnúkur volcano on August 23, 2024.

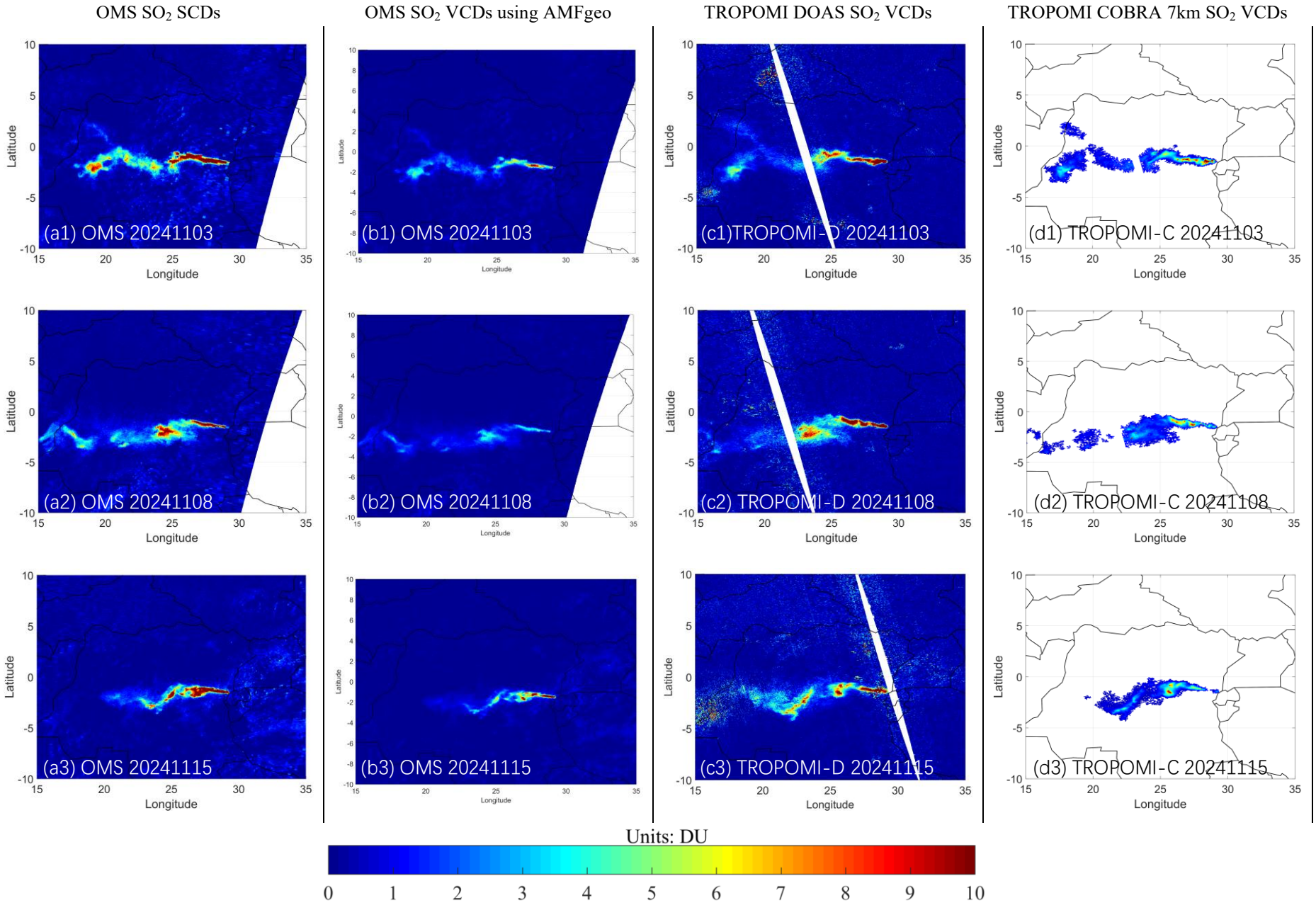

Figure: SO_2 retrievals of OMS and TROPOMI over the Nyamuragira volcano on November 3, 8, and 15, 2024.

OMS SO_2 SCDs

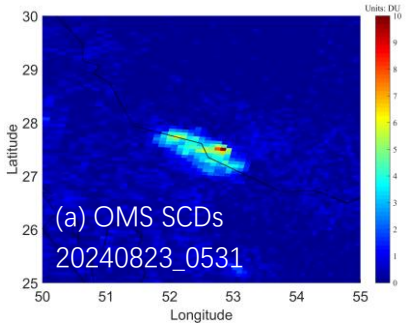

OMS SO_2 VCDs using AMFgeo

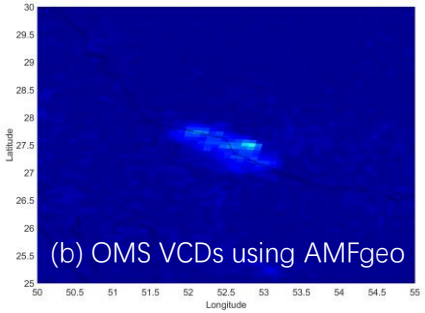

TROPOMI DOAS SO_2 VCDs

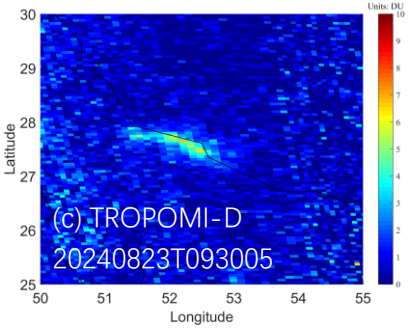

TROPOMI COBRA PBL SO_2 VCDs

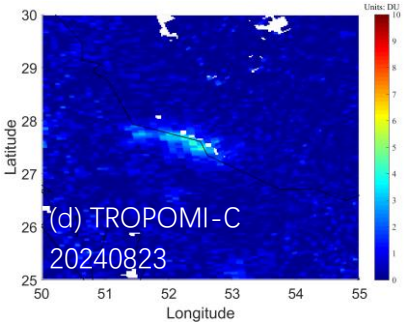

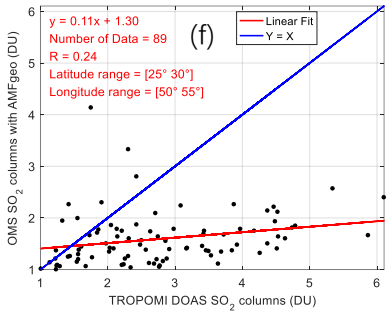

Figure: SO_2 retrievals of OMS and TROPOMI over the Persian Gulf on August 23, 2024.

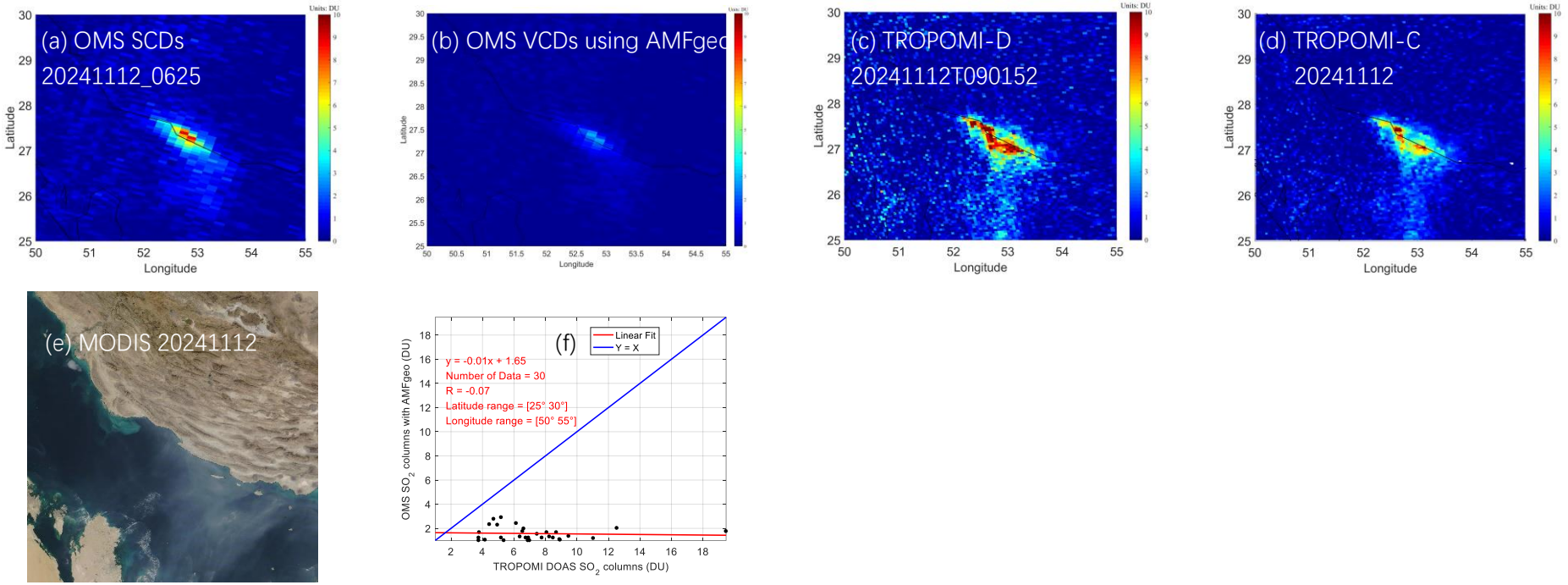

Figure: SO_2 retrievals of OMS and TROPOMI over the Persian Gulf on November 12, 2024.

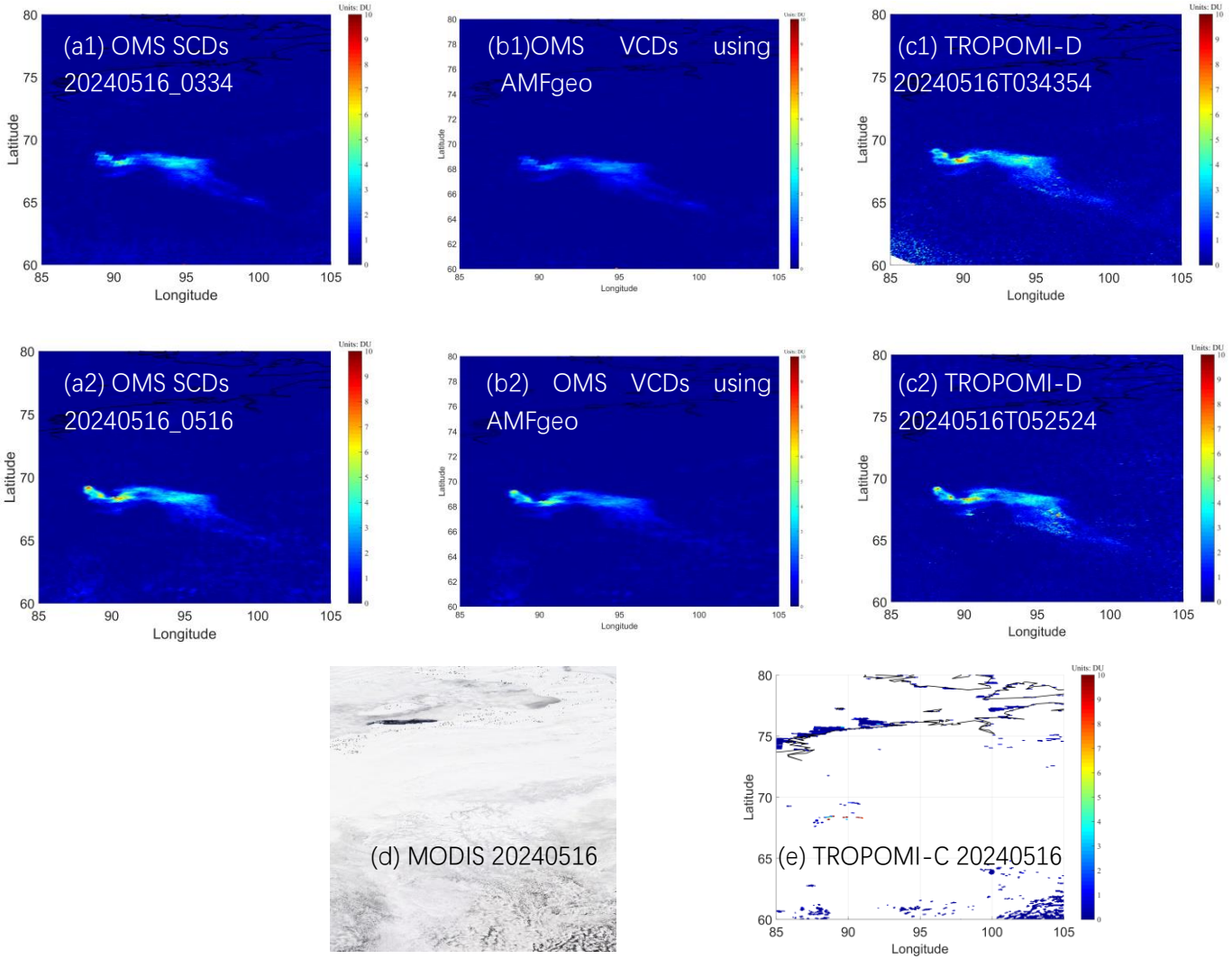

Figure: SO_2 retrievals of OMS and TROPOMI over Norilsk on May 16, 2024.

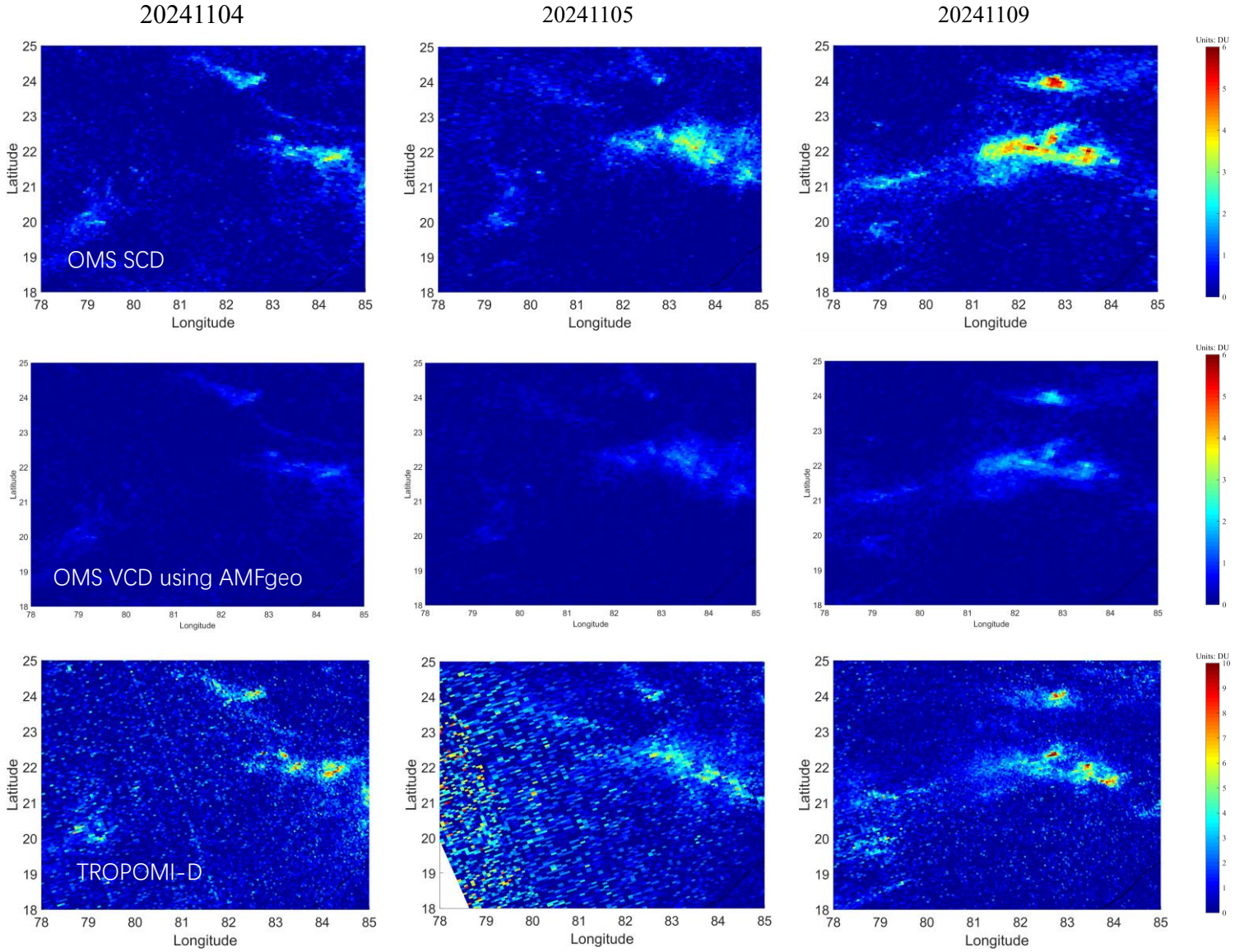
20241104
20241105
20241109
OMS SCD
OMS VCD using AMFgeo
TROPOMI-D
Latitude
Longitude
Units: DU

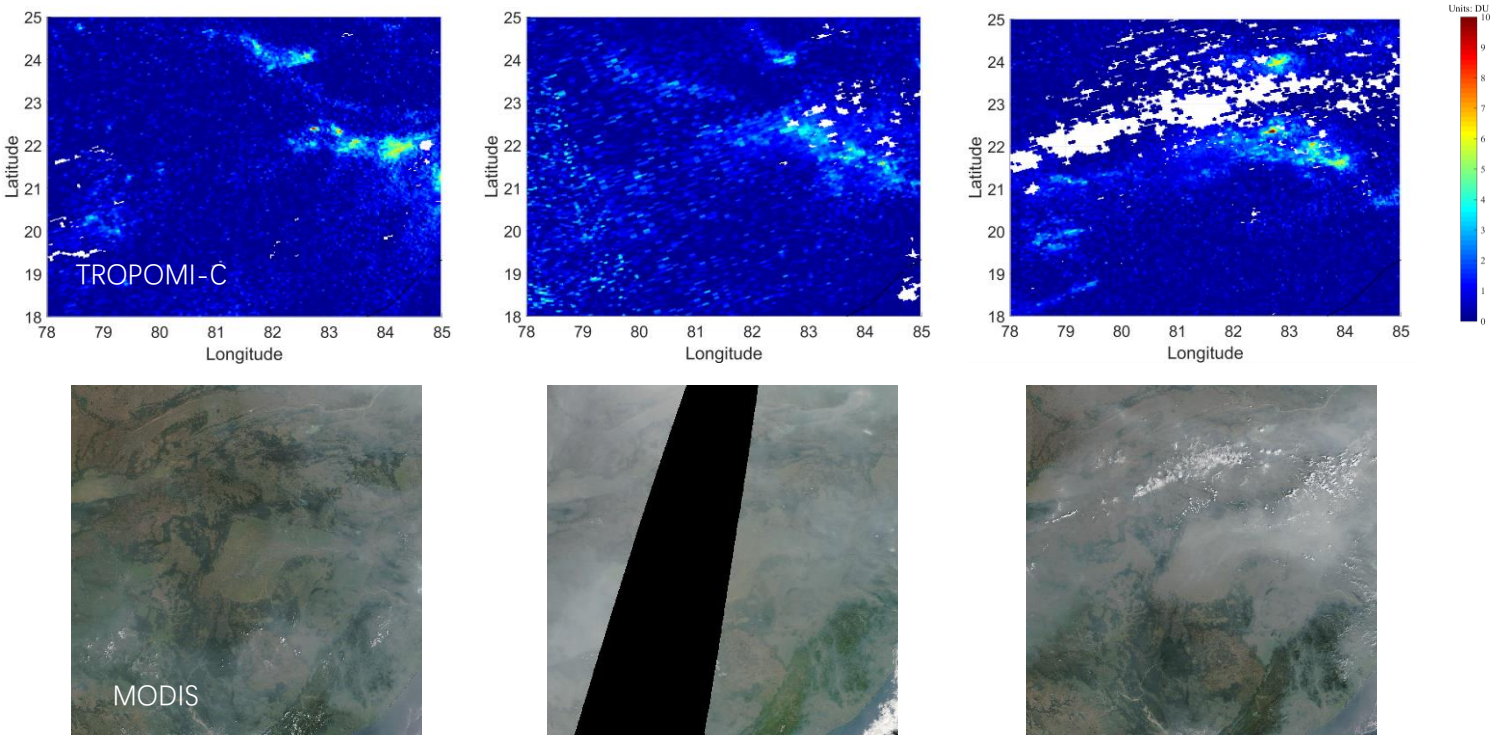

Figure: SO_2 retrievals over Eastern India on November 4, 5, and 9, 2024.

Supplement-2 (Employs RTM-based AMFs to convert OMS SO_2 SCDs to VCDs)

Region 1, Ocean-Area, 20240823

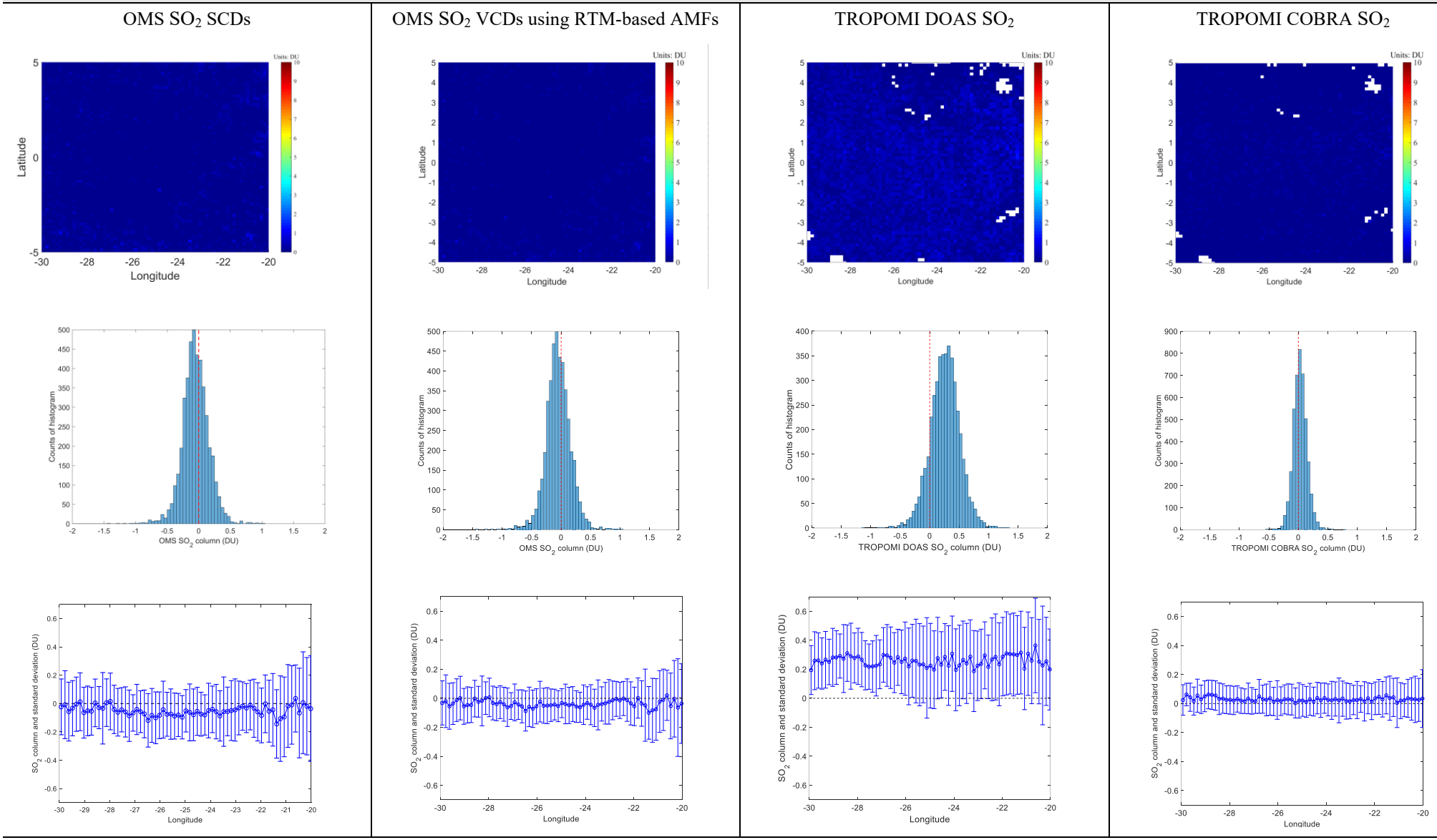

Figure 1: SO_2 retrievals over clean oceanic area (latitude from 5°S to 5°N and longitude from 30°W to 20°W, Region 1) on August 23, 2024. Note that OMS pixels with SO_2 column less than -10 and TROPOMI DOAS pixels with QA < 0.5 are assigned the value of -9999 and are not shown in the figure.

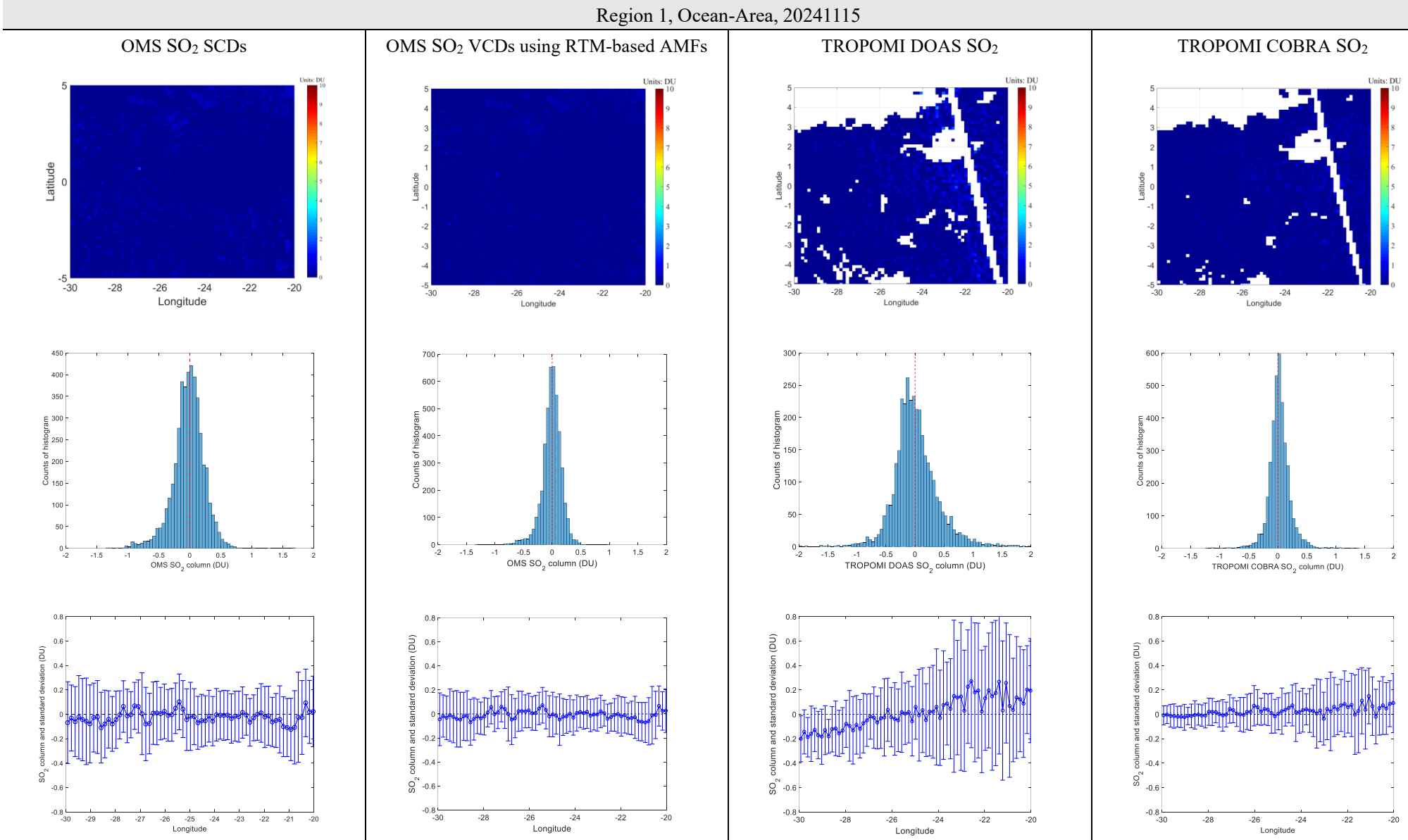

Figure 2: As Fig. 1 but for November 15, 2024.

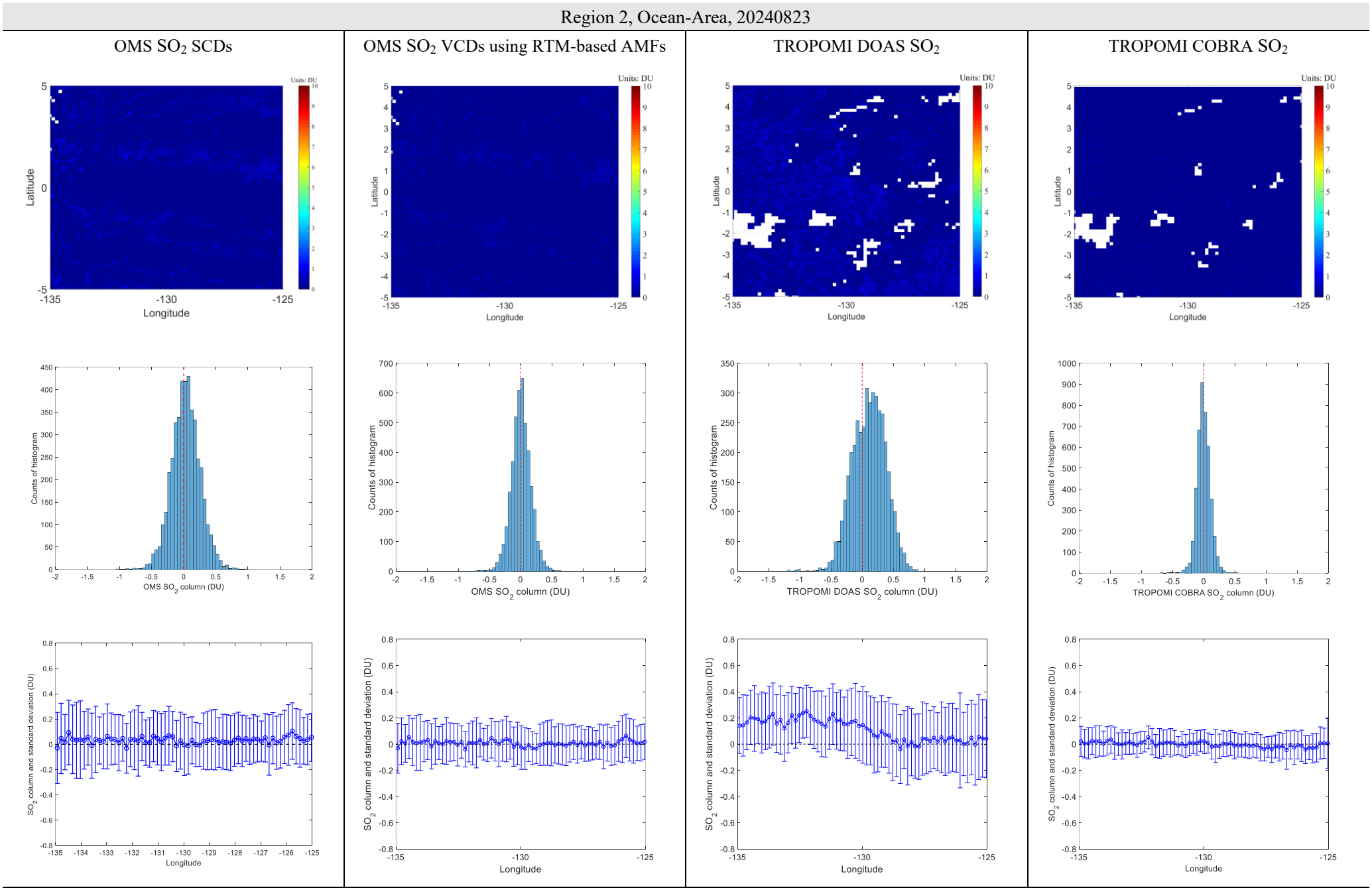

Figure 3: As Fig. 1 but for Region 2 (latitude from 5°S to 5°N and longitude from 135°W to 125°W).

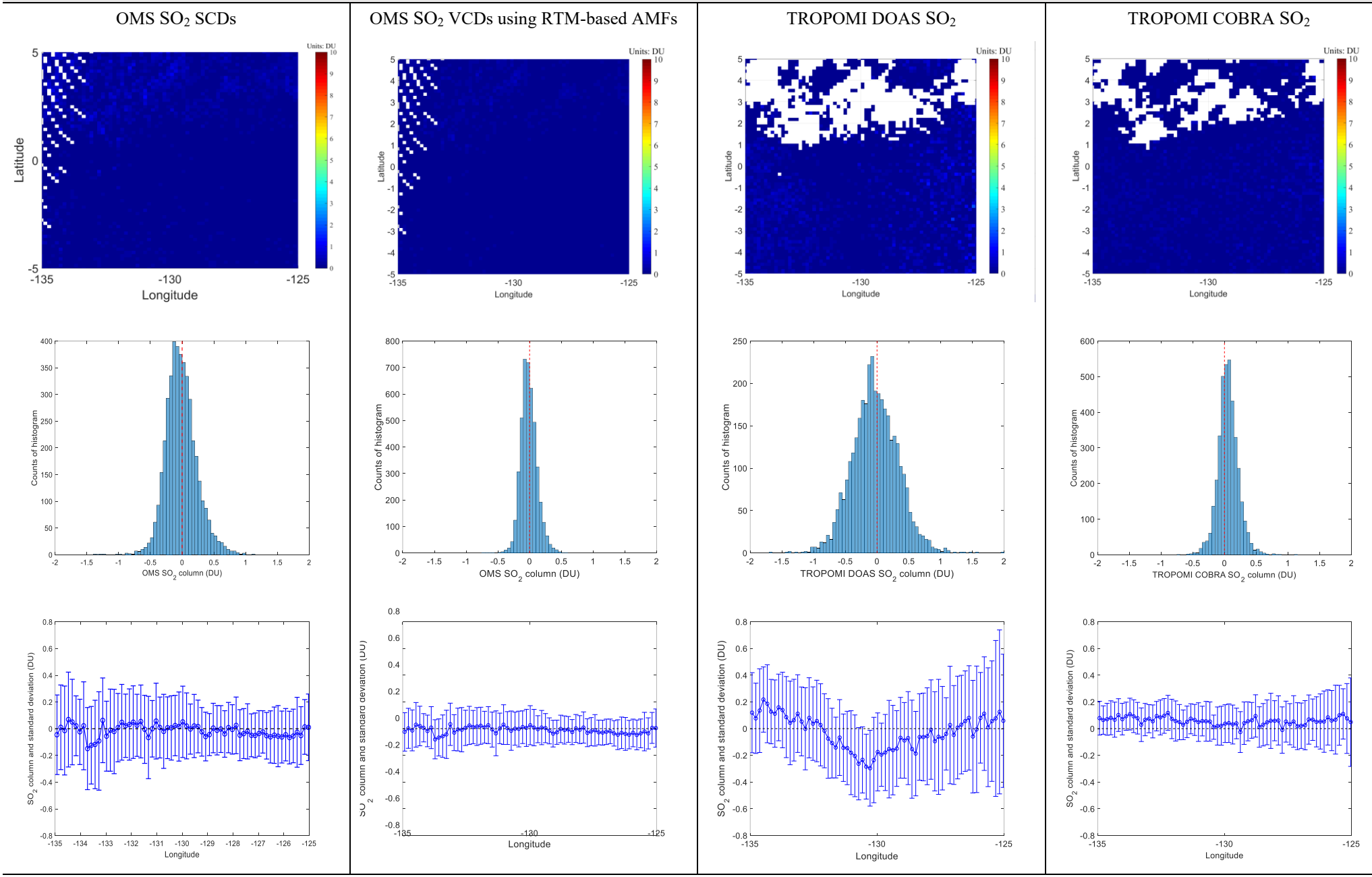

Figure 4: As Fig. 3 but for November 15, 2024.

OMS SO_2 SCDs (orbit 20240823_1217)

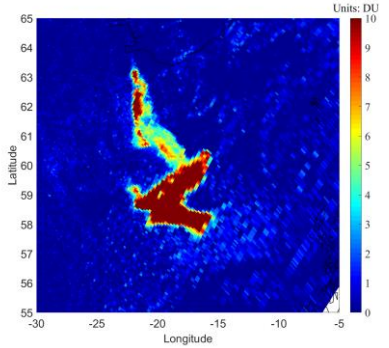

TROPOMI DOAS SO_2 (20240823T125304)

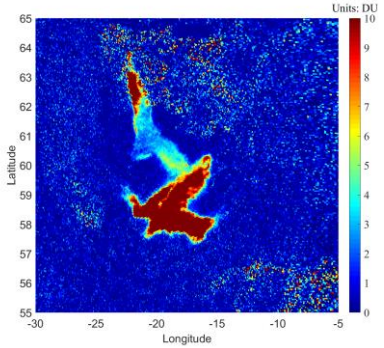

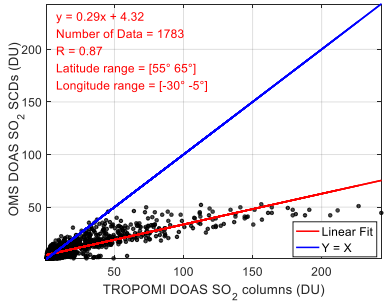

TROPOMI COBRA 7km SO_2 (20240823)

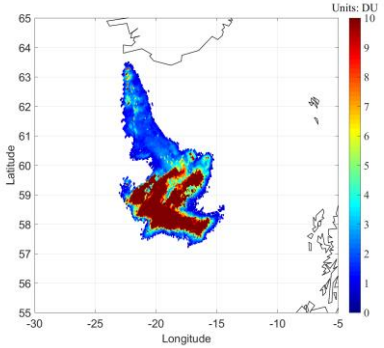

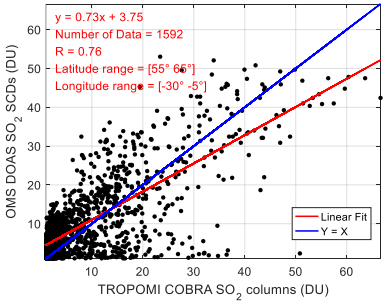

OMS SO_2 VCDs using RTM-based AMFs (orbit 20240823_1217)

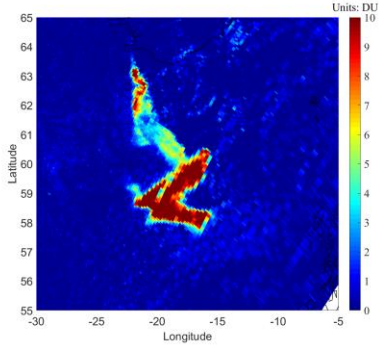

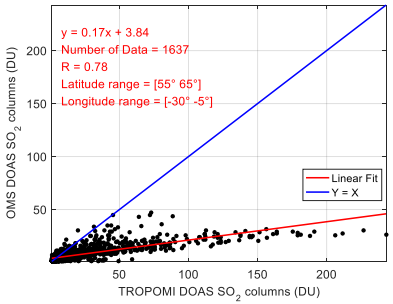

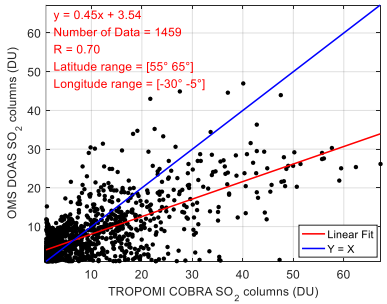

Figure 5: Spatial distribution and Scatter plots of FY-3F/OMS, TROPOMI DOAS and TROPOMI COBRA 7km SO_2 columns over Sundhnúkur volcano on August 23, 2024. Pixels with SO_2 columns greater than 1 DU were selected and TROPOMI is resampled to the latitude-longitude grid of OMS. The missing pixels in Figure OMS are the gap between the two OMS orbits, and the missing pixels in Figure COBRA are due to quality filtering applied to TROPOMI COBRA data.

OMS SO_2 SCDs	OMS SO_2 VCDs using RTM-based AMFs	Difference map between OMS SO_2 SCDs and VCDs using RTM-based AMFs	Scatter plot of OMS SO_2 SCDs and VCDs using RTM-based AMFs
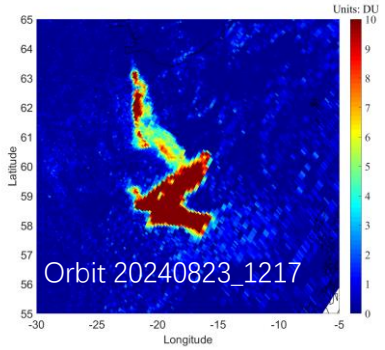	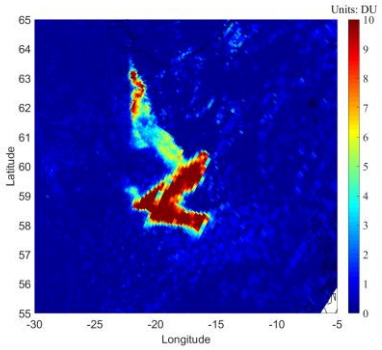	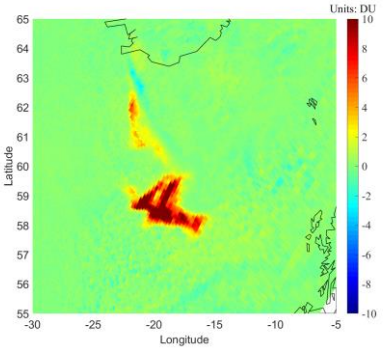	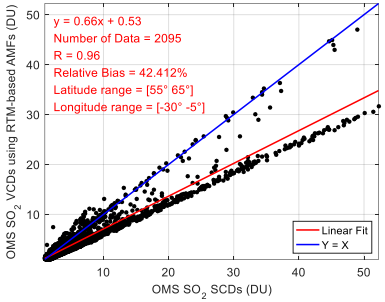
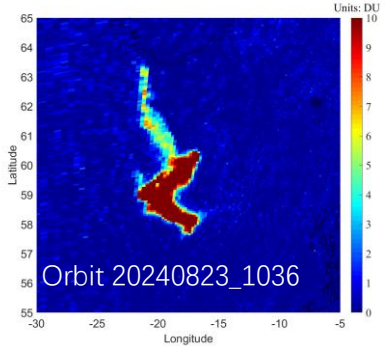	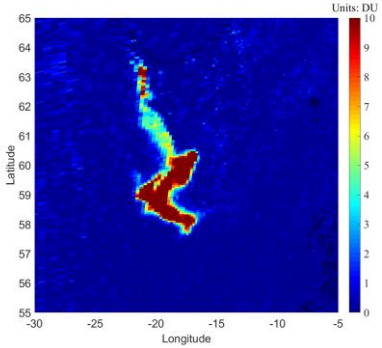	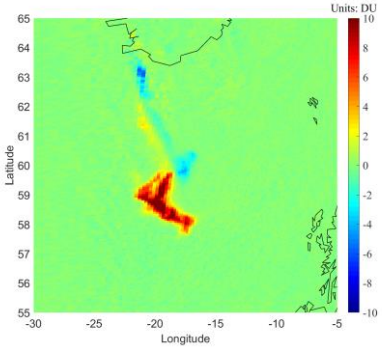	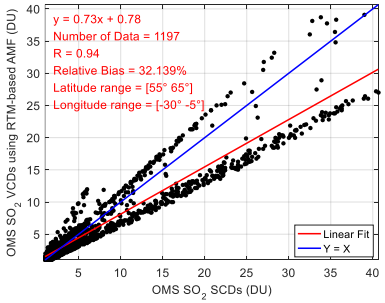

Figure 6: Comparisons of FY-3F/OMS SO_2 SCDs and VCDs using RTM-based AMFs over Sundhnúkur volcano on August 23, 2024.

OMS SO_2 SCDs	OMS SO_2 VCDs using RTM-based AMFs	TROPOMI DOAS SO_2	TROPOMI COBRA SO_2

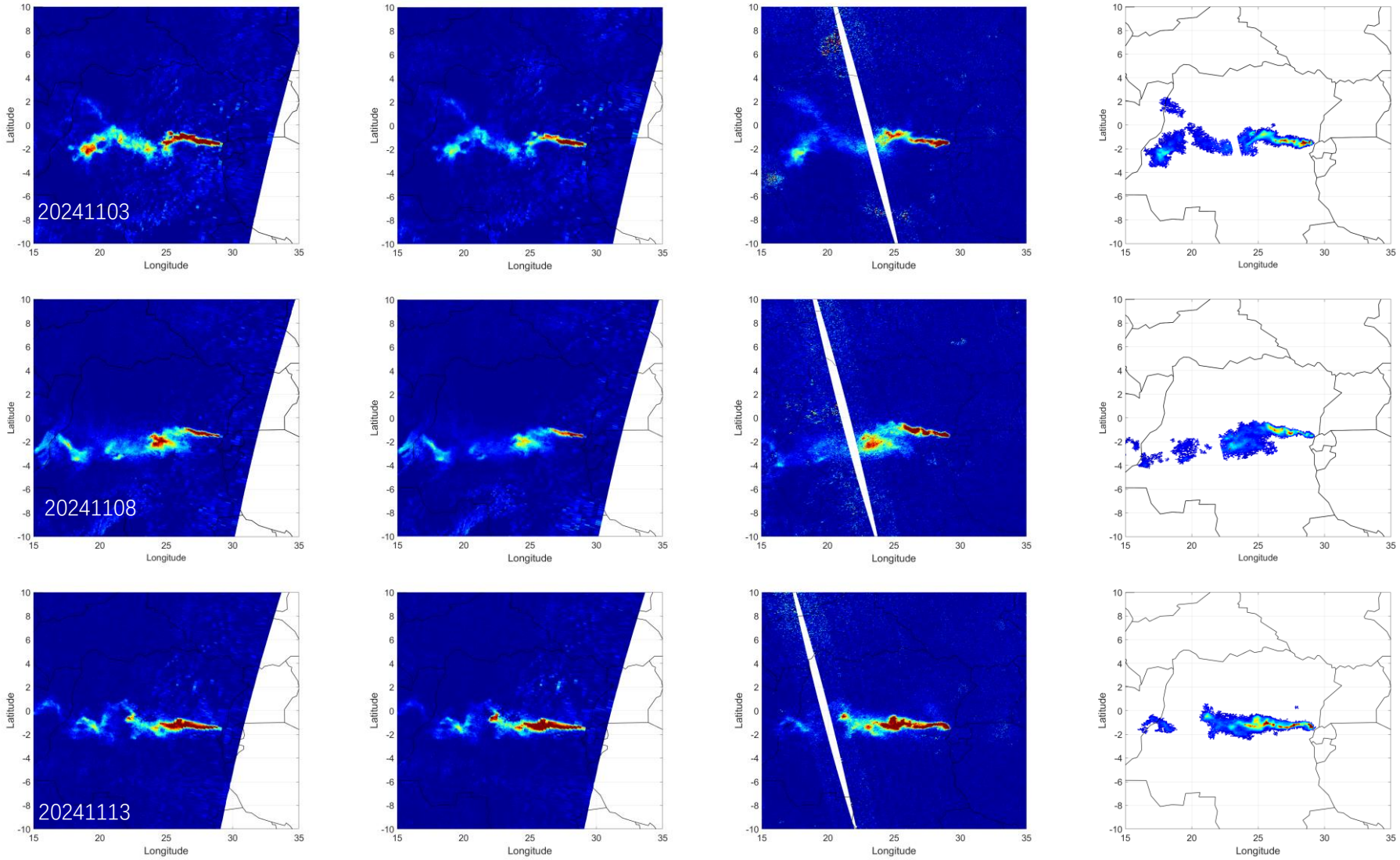

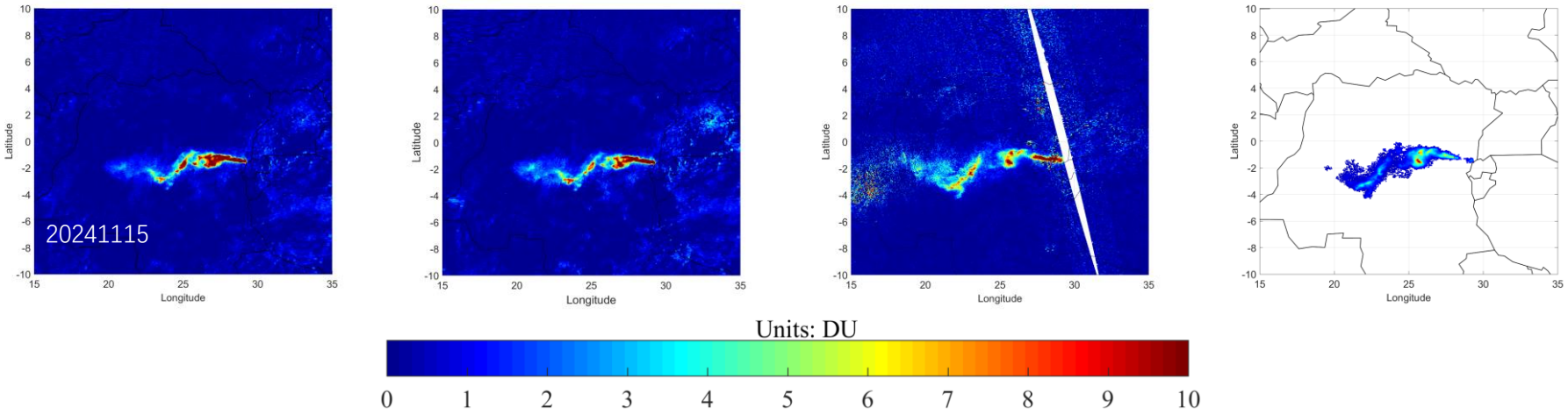

Figure 7: SO_2 retrievals of OMS and TROPOMI over the Nyamuragira volcano on November 3, 8, 13, and 15, 2024.

OMS SO_2 SCDs	OMS SO_2 VCDs using RTM-based AMFs	TROPOMI DOAS SO_2	TROPOMI COBRA SO_2

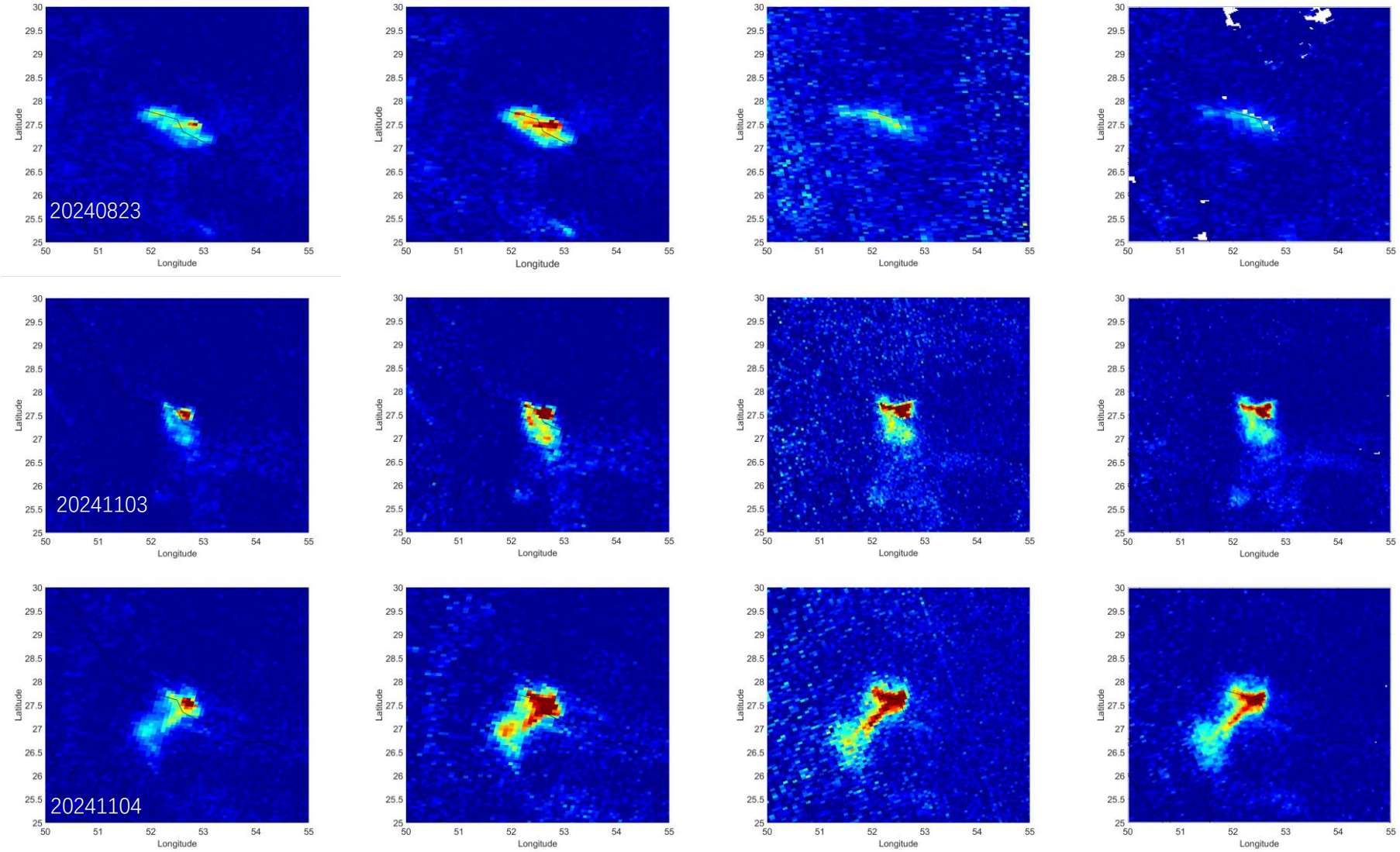

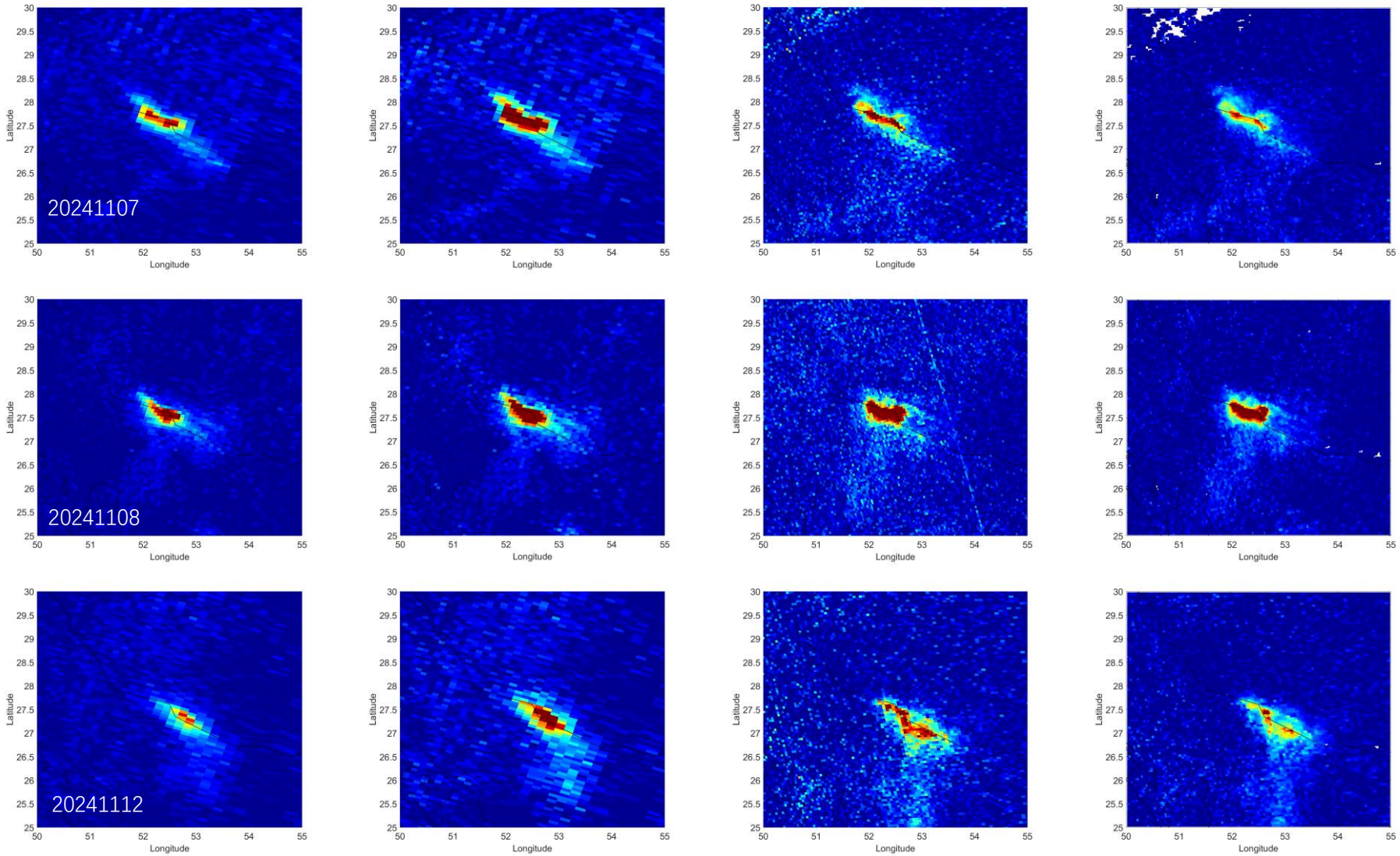
20241107
20241108
20241112
Latitude
Longitude

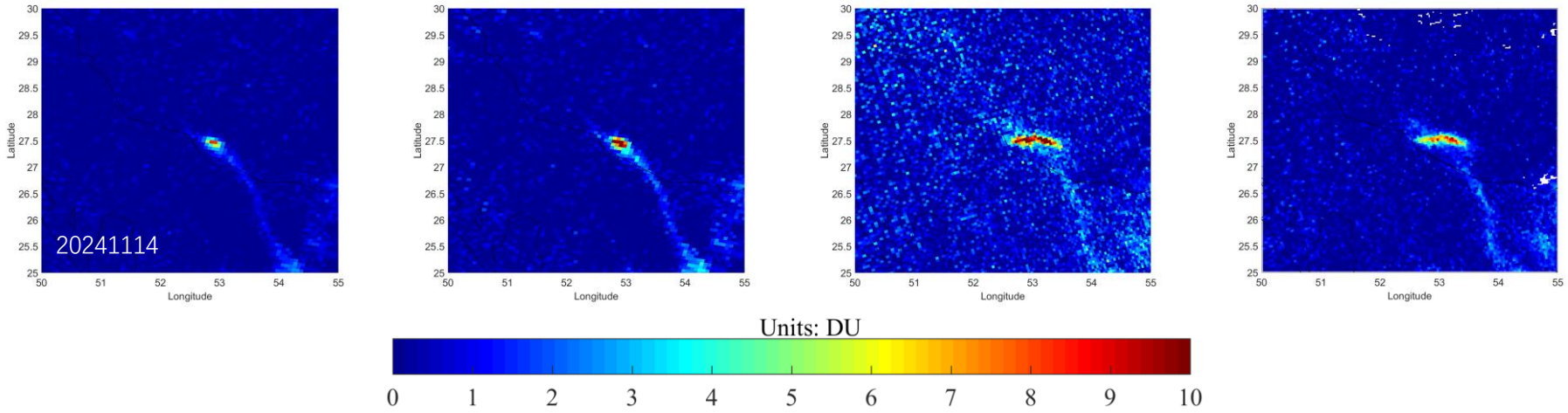

Figure 8: SO_2 retrievals of OMS and TROPOMI over the Persian Gulf on August 23, 2024, and November 3, 4, 7, 8, 12, and 14, 2024.

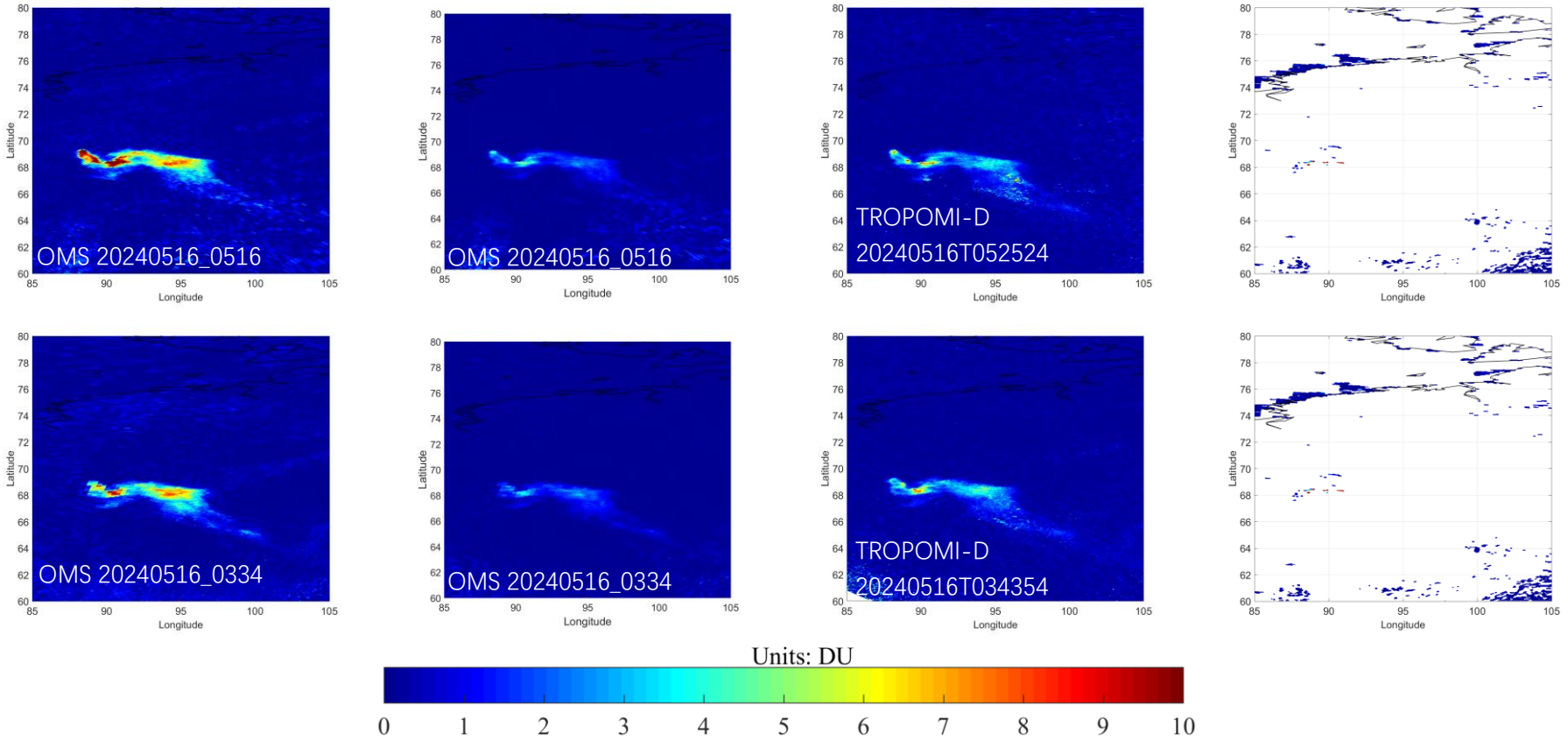

Figure 9: SO_2 retrievals of OMS and TROPOMI over Norilsk on May 16, 2024.

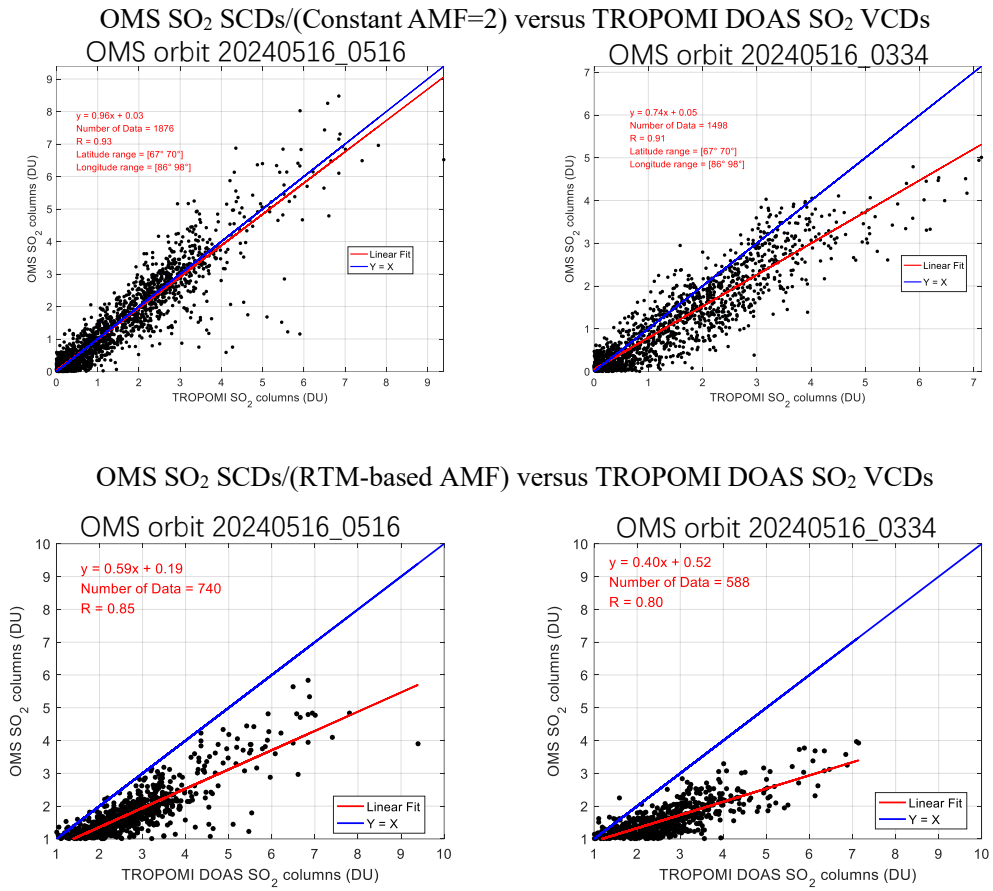

Figure 10: Scatter plot comparison between OMS SO_2 VCDs retrieved using different AMF strategies and the TROPOMI DOAS SO_2 product over Norilsk on 16 May 2024.

OMS SO_2 SCDs	OMS SO_2 VCDs using RTM-based AMFs	TROPOMI DOAS SO_2	TROPOMI COBRA SO_2
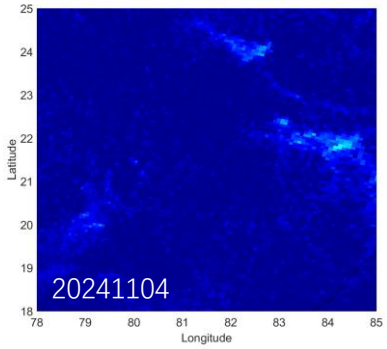	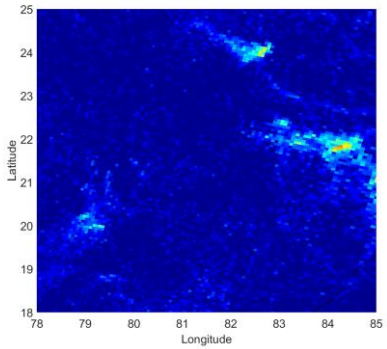	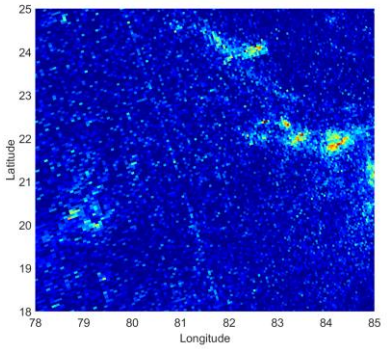	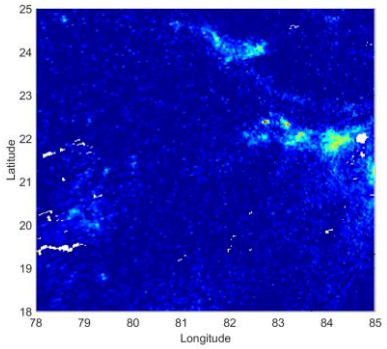
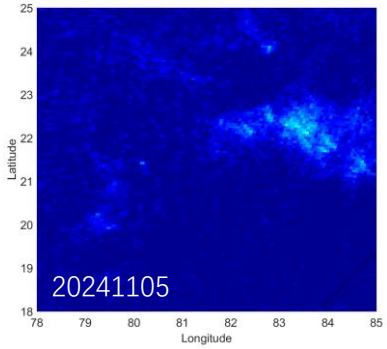	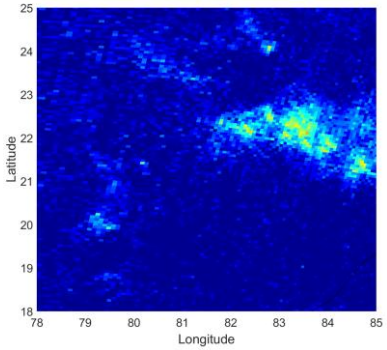	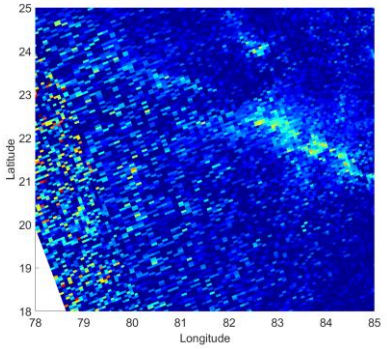	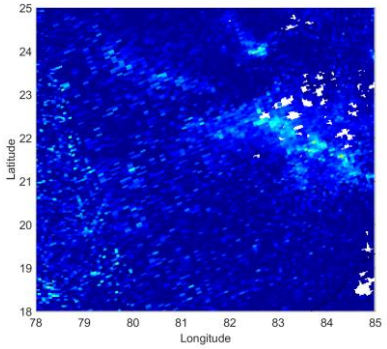
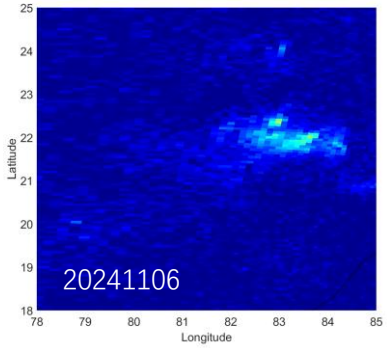	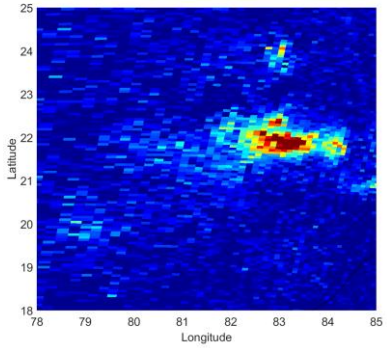	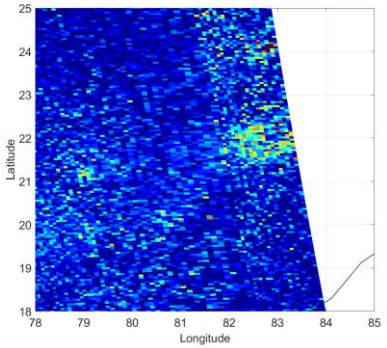	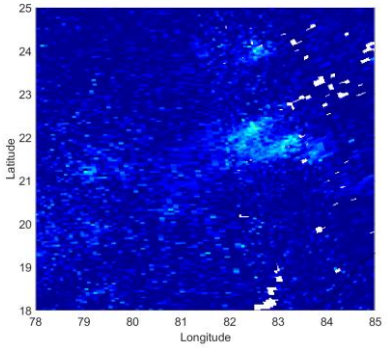

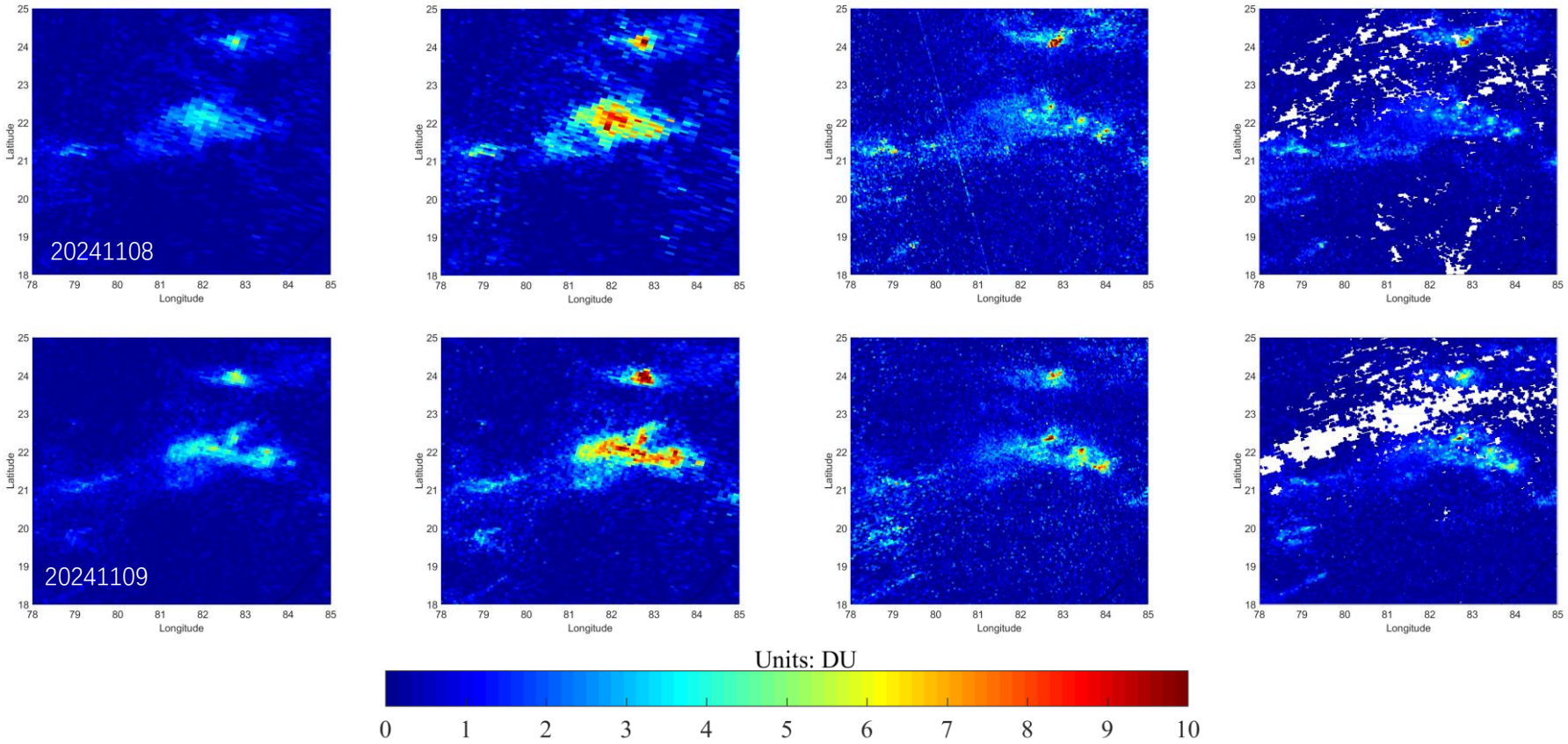

Figure 11: SO_2 retrievals of OMS and TROPOMI over Eastern India on November 4, 5, 6, 8, and 9, 2024.

Supplement-3

Hayli Gubbi is located near the southern end of the Erta-Ale volcanic range, a chain of volcanoes in the Afar region of eastern Ethiopia. It is a shield volcano that erupted on 23 November 2025, marking its first recorded eruption in approximately 12,000 years. Using FY-3F/OMS observations from 24, 25, and 26 November 2025, the spatiotemporal transport of SO_2 from this eruption was monitored. The results demonstrate that OMS successfully captured the transport pathway of the volcanic SO_2 plume. Under favorable meteorological conditions, SO_2-rich air masses were transported over long distances, sequentially affecting neighboring countries, India, China, and eventually the Pacific Ocean.

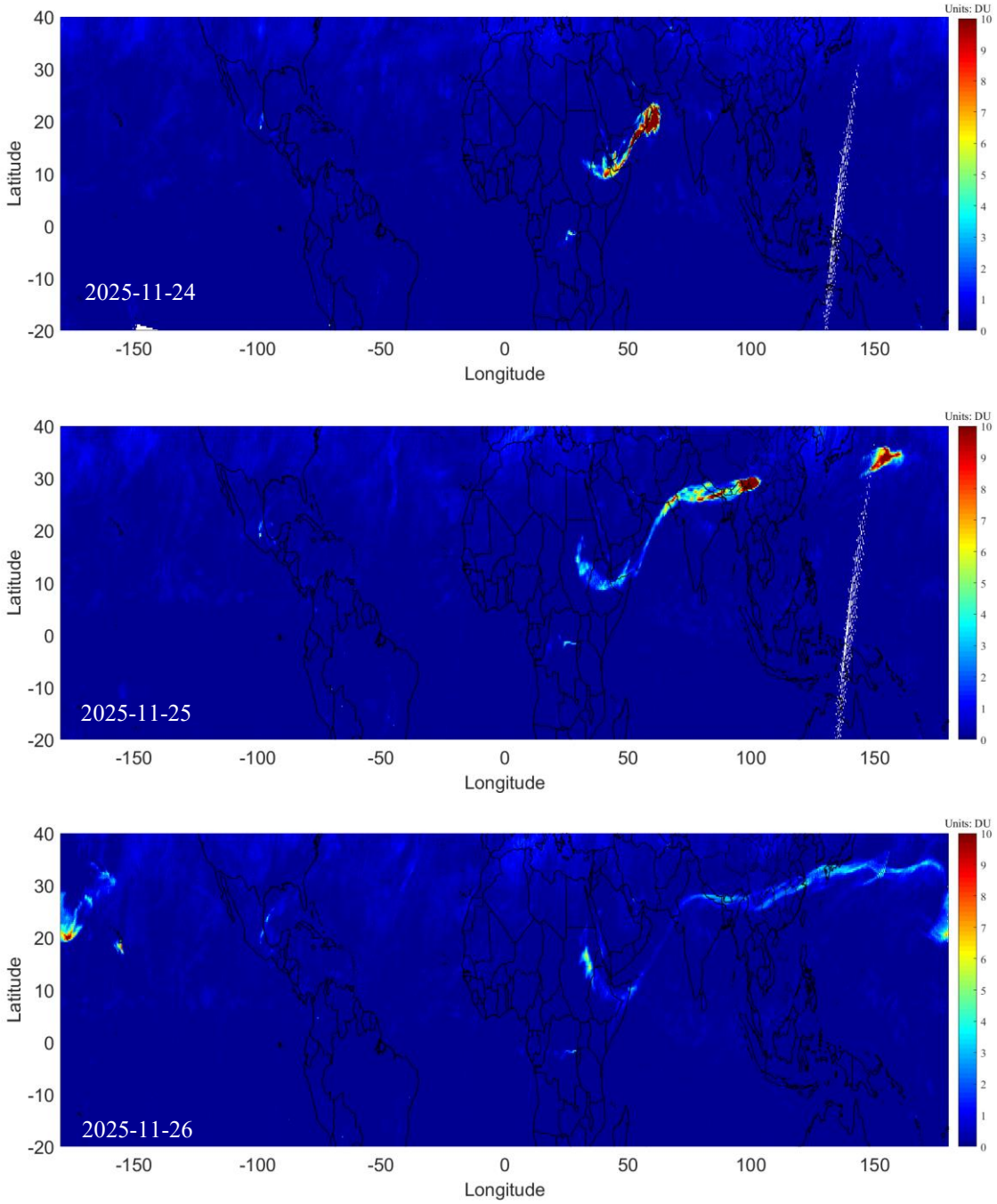

Figure: SO_2 SCDs retrieved from OMS over the Hayli Gubbi volcano on November 24, 25, and 26, 2025, gridded to a 0.3°×0.3° equal latitude-longitude grid.